

Harpur Hill, Buxton
Derbyshire, SK17 9JN
T: +44 (0)1298 218000
F: +44 (0)1298 218986
W: www.hsl.gov.uk



**Technical Assessment of Petroleum Road Fuel Tankers
Work Package 1 - Full scale testing and associated modelling
OVERALL SUMMARY**

ES/14/39/00rev05

Report Approved for Issue By:	Nigel Corlett, BEng(Hons), MSc, PhD, ACSM
Date of Issue:	26 November 2014
Lead Author:	Duncan Webb, BSc(Hons)
Contributing Author(s):	
Technical Reviewer(s):	Chris Atkin BEng(Hons) CEng MIMechE, James Hobbs MEng PhD, Alan McDonald BSc (Hons)
Editorial Reviewer (s):	Steven Williams
HSL Project Number:	PE05832

Disclaimer:

This report and the work it describes were undertaken by the Health and Safety Laboratory under contract to the Department for Transport. Its contents, including any opinions and/or conclusion expressed or recommendations made, do not necessarily reflect policy or views of the Health and Safety Executive.

DISTRIBUTION

Steve Gillingham	Principal Engineer, Department for Transport
Nigel Corlett	HSL, Head of Engineering and Personal Safety
Author	
Duncan Webb	HSL Project manager
HSL Reports and papers	pdf only
Library	

Technical Assessment of Petroleum Road Fuel Tankers

Disclaimer

Certain aspects of this report, and any results and conclusions set out within it, may be disputed by the tank manufacturer.

Report Approved for Issue by:	Nigel Corlett, BEng(Hons), MSc, PhD, ACSM
Date of issue:	26 November 2014
Lead Author:	Duncan Webb, BSc(Hons)
Contributing Author(s):	
HSL Project Manager:	Duncan Webb, BSc(Hons)
Technical Reviewer(s):	Chris Atkin BEng(Hons) CEng MIMechE, James Hobbs PhD, Alan McDonald BSc(Hons)
Editorial Reviewers:	Steven Williams
HSL Project Number:	PE05832

CONTENTS

LIST OF FIGURES.....	iii
LIST OF TABLES	iv
1 INTRODUCTION	1
2 ASSESSMENT AND SUPPLY OF TANKERS.....	3
2.1 Tankers used in the research programme	3
2.2 GRW tanker design and construction	4
2.3 Selection of GRW tankers for tests and radiography	5
2.4 Radiography of GRW tankers	6
2.5 Damaged GRW tankers.....	8
3 TANKER TOPPLE TEST METHODS AND RESULTS	9
3.1 Methods.....	9
3.2 Results.....	13
3.3 Test uniformity and use of test data for HSL's finite element model	22
4 MODELLING TO PROVIDE LOAD CASE DATA FOR ROLLOVER	23
4.1 Initial development of the tanker rollover model.....	23
4.2 Refinement and validation of the tanker rollover model	24
4.3 Modelling real-world fuel loads	32
4.4 Output for WP2 Engineering Critical Assessment.....	36
5 CONCLUSIONS	39
6 REFERENCES	42

last page = 42

List of Figures

Figure 1	8-banded 6-compartment GRW tanker - bulkheads and baffles.....	4
Figure 2	10-banded 6-compartment GRW tanker - bulkheads and baffles.....	4
Figure 3	Schematic of radiograph starting positions for GRW 8-banded tanker	7
Figure 4	Nearside of GRW tanker J2580 with hose tray	7
Figure 5	Damage to the rear of GRW tanker J3217.....	8
Figure 6	Laser scan image of the rear GRW tanker J3217.....	8
Figure 7	The key features of the HSL tanker topple test.....	9
Figure 8	Location of instrumentation on GRW tankers J2580 and J3910	11
Figure 9	High speed video images during impact – GRW tanker J2580	15
Figure 10	High speed video images during impact – GRW tanker J3910.....	16
Figure 11	Comparison - pressure measured at the centre of the impact area.	17
Figure 12	Comparison - longitudinal strain near rear bulkhead in C1b and C4	18
Figure 13	GRW tanker J3910 - impact damage viewed from front.....	19
Figure 14	GRW tanker J2580 – rupture in the weld at top of impact zone	20

Figure 15	GRW tanker J2580 – apparent through-wall crack along the circumferential weld at the top of the impact zone at the rear (band H/8)	20
Figure 16	GRW tanker J3910 – rupture at toe of weld at top of impact zone	21
Figure 17	GRW tanker J3910 – crack at toe of weld at bottom of impact zone	22
Figure 18	Overview of GRW tanker finite element model.....	25
Figure 19	Fillet welds, GRW tanker J3910, Band B/8-	26
Figure 20	Band extrusion profile for GRW tanker J2580.....	26
Figure 21	Band extrusion profile for GRW tanker J3910.....	27
Figure 22	Comparison of flat lengths at band locations for GRW tanker J3910 test and finite element model data	28
Figure 23	Comparison of bending moments near band B for GRW tanker J3910 test and finite element models	29
Figure 24	Comparison of bending moments at centre of C1b for GRW tanker J3910 test and finite element models	30
Figure 25	Comparison of pressures near the impact location in C1b for GRW tanker J3910 test and finite element model data.....	31
Figure 26	Plastic strain in the bulkheads from the J3910 modified finite element model	31
Figure 27	Effect of tanker load (fuel oil/water/petrol) on deformation (band deflections) at 2.0 rad/s impact velocity	33
Figure 28	Bending moments near to band E showing large differences.....	34
Figure 29	Bending moments near to band F	34
Figure 30	Deformed bulkheads for fuel oil finite element model with impact at 2.6 rad/s clearly showing effect of pressure only on the convex side of bulkhead D	35
Figure 31	Deformed bulkheads due to petrol impact at 2.0 rad/s	35
Figure 32	Bending moments per unit length at the rear of the tanker shell under fuel oil loading conditions at 2.0 rad/s.....	37
Figure 33	Bending moments next to Band F/8+ showing variation due to fuel	37
Figure 34	Variation in bending moments with distance from the weld (Band F/8+) for water (2.0 rad/s), fuel oil (2.6 rad/s) and petrol (2.0 rad/s)	38
Figure 35	Variation in bending moments with distance from the rear weld (Band H+) for water at 1.89 rad/s	38

List of Tables

Table 1	List of related HSL reports for Work Package 1	2
Table 2	GRW tankers considered for the research programme “Technical assessment of petroleum road fuel tankers”	3
Table 3	List of models created	23
Table 4	Model-to-test correlation - bending moments and membrane stresses near the band with differences expressed as percentage of test result and as percentage of yield stress	29
Table 5	Model-to-test correlation - bending moments and membrane stresses at the compartment centres with differences expressed as percentage of tests results and as percentage of yield stress.....	30
Table 6	Maximum plastic strains in the bulkheads for different load liquids.....	32

EXECUTIVE SUMMARY

Background

Following examination, certain petroleum road fuel tankers have been found to not be fully compliant with the provisions of Chapter 6.8 of the European Agreement on the Carriage of Dangerous Goods by Road (ADR). Amongst other things, these tankers are seen to exhibit extensive lack-of-fusion defects in the circumferential weld seams which, based on a leak-before-break assessment¹, could rupture under rollover and ADR load conditions.

The Department for Transport (DfT) commissioned research consisting of three work packages (WPs):

- WP1 – Full scale testing and associated modelling; Health and Safety Laboratory (HSL).
- WP2 – Detailed Fracture and Fatigue Engineering Critical Assessment (ECA); TWI Ltd.
- WP3 – Accident data and regulatory implications, and production of an overall summary report of the research; TRL Ltd.

HSL has taken forward the tasks set out in WP1 to:

1. Develop an independent non-proprietary structural hydrodynamic model of GRW tankers, validate this model against the results of tanker tests, and report modelling findings.
2. Design, construct and commission a test rig for tests of tankers, including selecting and procuring suitable instrumentation for data gathering.
3. Undertake tests on tankers, including preparing the tankers, assessing the tanker test method and results, and reporting the findings.
4. Determine suitability of tankers for large scale tests and acquire tankers, as appropriate, in accordance with project objectives as specified by DfT.
5. Capture collision and/or deformation data from relevant impacts, for example by laser scanning, to corroborate the modelling and tanker tests, and reconcile any inconsistencies.
6. Engage in peer review activities on the overall DfT research programme.

This report summarises the findings of the combined outputs from the work undertaken in WP1.

Overall findings

The test outcomes demonstrated that the topple test was a reliable test method providing repeatable test data suitable for validating HSL's Finite Element (FE) modelling. The impact velocities for the GRW tanker tests lay within the range reported for real-world rollovers.

Overall, HSL's finite element model of the HSL topple test with a water load for GRW tanker J3910 correlated well with the topple test data, providing good validation of the model.

The highest levels of plastic strain in the finite element model with a water load were observed in the bulkheads, at the top and bottom of the flat generated by the impact. The magnitude of the peak plastic strains was in the order of 0.2 (or 20%), a level at which failure may occur. It was at the top of this flat where ruptures in the toe of the weld and within the weld between the extrusion band and the bulkhead occurred during the topple tests on GRW tankers J2580 and J3910, respectively.

¹ 'Short-term Fitness for Service Assessment of [non-compliant] Road Tankers, TWI (Draft) Report 23437/1/13, September 2013 and 'Project 23437 Contract Amendment: Additional FEA for assessment of [non-compliant] road tankers, TWI (Draft) Report 23437/2/13, October 2013.

Assessment and supply of tankers

The objectives of this part of the work were to:

- Facilitate, as required by DfT, the selection, inspection and procurement of tankers to be used by HSL and other consortium members in the delivery of the project.
- Capture data, including physical samples if needed, from damaged tankers where these data or samples may be useful in the research.

Main Findings - Assessment and supply of tankers

The primary criteria for GRW tanker selection, for both the topple tests (WP1) and the fatigue data collection activities (WP2) were:

- that the tanker should be representative of ‘in-service’ UK-based GRW tankers; and
- the condition, based on radiography, of the tanker’s circumferential welds to ensure the tests included a range of weld qualities of tankers as found in service.

The circumferential welds of ten² 8- and 10-banded GRW tankers manufactured between 2007 and 2011 were radiographed (four prior to the project). The results of the radiography both informed the selection of tankers for the topple and road tests, and provided information on the condition of the welds in a range of GRW tankers manufactured over a five-year period. Two 8-banded 6-compartment tankers, J2580 and J3910, were selected for topple tests. One 10-banded 6-compartment tanker, J3857, was selected for road tests to gather fatigue data in WP2. The radiography for J3910 showed the highest proportion of lack of fusion indications in the welds, whilst J3857 and J2580 showed the lowest.

The GRW tankers selected for test were all fully ADR inspected and, where necessary, remedial work was conducted to ensure that the tankers satisfied the test requirements, and were roadworthy and loadworthy. In addition, the GRW tankers selected for topple test were subject to a second radiography examination, and to internal surveys of the fillet welds. GRW tanker J3910 was subject to an additional internal survey of circumferential weld misalignment, and an external laser scan survey of the circumferential weld caps. General design and construction differences between 8- and 10-banded tankers, which were relevant to the research, have been established. Specific design and construction differences, due to changes in GRW design and welding process, between GRW tankers J2580 and J3910 were found in the extrusion profiles, the bulkhead (or baffle) welding to the extrusion bands and the fillet welds.

A suitable 8-compartment 40,000 litre petroleum road tanker of aluminium construction in roadworthy and loadworthy condition was sourced for the proof of concept topple test. Two damaged GRW tankers, J3217 with rear damage and J3146 with front damage, were laser scanned for dimensional information on the damage, with physical samples taken, for WP2 use.

Tanker topple test methods and results

The objectives of this part of the work were to:

- Design, construct and commission a test rig for tankers which offers a reliable and repeatable method to provide experimental data for use in both improving the understanding of tanker impact behaviour and validating HSL’s finite element modelling.
- Prepare and test tankers to provide experimental data for use in both improving the understanding of tanker impact behaviour and validating HSL’s finite element modelling.

Main Findings - Tanker topple test methods and results

Overall, the outcomes of a proof of concept test and tests on two GRW tankers, J2580 and J3910, demonstrated that the topple test was a reliable test method providing repeatable test data suitable for validating HSL’s finite element modelling.

² one further tanker may be added to the list in a revision of this report

HSL developed a topple test with a water load whereby a prepared tanker was tilted under controlled conditions until it became unstable and fell onto its offside under the influence of gravity. GRW tankers were instrumented with pressure transducers, strain gauges and accelerometers to record data for the impact, logged at 50,000 samples per second (or one sample every 0.02 millisecond). Tests were recorded using thirteen video cameras ranging from standard speed (25 frames per second) to high speed (1,000 frames per second).

GRW tankers J2580 and J3910 were filled to be at, or very close to, their maximum rated load mass (31,380 kg), which was below their rated volume for fuel. Both were filled with 31,376 litres of water (31,376 kg), with each of their compartments filled to about 70% of its maximum capacity. The impact velocities for the GRW tanker tests were between 1.82 and 1.93 rad/s, values which lie within the range of 1.75 to 2.62 rad/s reported for real-world rollovers. The offside of the tanker impacted uniformly along its length, with less than 7 ms between the impact of the front and rear for the GRW tankers.

After the test, the offside (impact side) of the GRW tankers exhibited a similar deformation shape with the impact area flattened. The deformation profile was similar along the length of the tankers, with the level of deformation increasing from front to rear. The deformation data, both as a reduction in tanker diameter and as the chord length of the flat section, were similar for the GRW tankers. The impact caused a permanent reduction in tanker diameter of approximately 100 mm at the rear and 82 mm at the front of GRW tanker J2580, and of approximately 107 mm at the rear and 82 mm at the front of GRW tanker J3910.

GRW tankers J2580 and J3910 both ruptured during impact. There was a visible leak from GRW tanker J2580 between the rear bulkhead and extrusion band at the top of the impact area. Subsequent visual inspection found a rupture within the weld between the rear bulkhead and extrusion band at the top of the impact area, and no visible damage at the bottom of the impact area. Pneumatic pressure tests found that all compartments in GRW tanker J2580 had lost their internal integrity. HSL supplied TWI with samples from GRW tankers J2580 and J3910 for post-mortem assessment under WP2. During post-mortem examination, TWI observed an apparent through-wall crack along the circumferential weld at the top of the impact zone for the sample including the impact zone from the off-side rear of GRW tanker J2580. This apparent crack can be seen on close examination of HSL photographs of the tanker after being lifted back onto its wheels. Detailed fractographic analysis of the J2580 and J3910 samples is addressed in the WP2 report. GRW have indicated that the damage around the joints between the extrusion band and the bulkhead/baffles for both tankers is consistent with real-world rollovers.

There was a visible leak from GRW tanker J3910 between the front bulkhead and the extrusion band at the top of the impact area. Subsequent visual inspection found a rupture in the toe of the weld between the front bulkhead and the extrusion band at the top of the impact area, and a crack in the toe of this weld at the bottom of the impact area. Pneumatic pressure tests of GRW tanker J3910 found that internal integrity had been lost between compartments 1 and 2 and between compartments 4 and 5, while the other bulkheads and compartments had maintained their internal integrity.

Modelling to provide load case data for rollover

The objective of this part of the work was to:

- Create and validate a structural hydrodynamic model of GRW tankers under rollover conditions.

and, in particular to:

- Create an original representative tanker rollover model which includes impact with the ground, realistic fluid motion and rotational velocity, refining an existing HSL structural

model of a partial tanker to represent a full GRW tanker so that transverse loading can be modelled.

- Refine the structural hydrodynamic model of the GRW tanker to describe GRW tankers J2580 and J3910 which were topple tested by HSL.
- Validate a suitably refined GRW tanker finite element model against topple test data.
- Apply the validated GRW tanker finite element model to a real-world fuel load representative of real-world conditions and consider the model outputs.

Main Findings - Modelling to provide load case data for rollover

Overall, HSL's finite element model of the HSL topple test with a water load for J3910 correlated well with the topple test data for GRW tanker J3910, providing good validation of the model. There were only small differences between the finite element model results for J2580 and J3910. This was a similar outcome to the topple test results, which were very consistent between the tests of GRW tankers J2580 and J3910. The highest levels of plastic strain in the finite element model with a water load were observed in the bulkheads, at the top and bottom of the flat generated by the impact, with peak magnitudes in the order of 0.2 (or 20%), a level at which failure may occur. It was at the top of this flat where ruptures in the toe of the weld and within the weld between the bulkhead and extrusion band occurred during the topple tests on GRW tankers J2580 and J3910, respectively.

The orientation of the bulkhead curvature was found to have a large effect on the bending moments in the tanker shell near to the extrusion bands. In simple terms, the bending moments were higher on the convex side of the bulkheads. Although the resolution of the model was not sufficient to consider the extrusion bands and welds in detail (this detail was considered in WP2), fillet welds were found to affect behaviour near to the extrusion bands. Impact velocity within the ranges modelled (1.89 to 2.0 rad/s for water, 2.0 to 2.6 rad/s for fuel oil and 2.0 rad/s for petrol) did not have a major influence on the results from the finite element models.

The fuel oil case modelled the tanker with one compartment empty, as occurs in practice because fuel oil has higher density than petrol. Modelling a tanker with a representative load of fuel oil or petrol, as opposed to water in all compartments, led to significantly higher deformation at the front of the tanker for petrol, and at the rear of the tanker for both fuels. Pressures, stresses and bending moments for the fuel oil and petrol models were also higher at the rear of the tanker than for the water model. The most significant feature for fuel oil was the behaviour around the empty compartment, with considerable differences when compared to the water model. The fuel load models suggest that the topple test conditions, with a water load distributed evenly throughout the tanker, may not be as severe as some real-life events.

Using the 2.6 rad/s fuel oil model, single values for bending moment (1460 N·mm/mm) and membrane stress (21.5 MPa) at the front side of the rear extrusion band in compartment 4 were extrapolated from model elements close to the circumferential weld. Extrapolating the same way using the 1.89 rad/s water model gave bending moments up to 1500 N·mm/mm for the location on the rear circumferential weld of compartment 6 corresponding to the through-wall crack in GRW tanker J2580. These values were supplied to WP2 for the detailed ECA. The limiting effect of the plastic strains in the shell means that other loading scenarios would be unlikely to give significantly different results.

1 INTRODUCTION

This work has been conducted as part of the Department for Transport's (DfT) technical assessment of petroleum road fuel tankers.

Following examination, certain petroleum road fuel tankers have been found to not be fully compliant with the provisions of Chapter 6.8 of the European Agreement on the Carriage of Dangerous Goods by Road (ADR). Amongst other things, these tankers are seen to exhibit extensive lack-of-fusion defects in the circumferential weld seams which, based on a leak-before-break assessment³, could rupture under rollover and ADR load conditions.

The Department for Transport (DfT) commissioned research consisting of three work packages (WPs):

- WP1 – Full scale testing and associated modelling; Health and Safety Laboratory (HSL).
- WP2 – Detailed Fracture and Fatigue Engineering Critical Assessment (ECA); TWI Ltd.
- WP3 – Accident data and regulatory implications, and production of an overall summary report of the research; TRL Ltd.

HSL has taken forward the tasks set out in WP1 to:

1. Develop an independent non-proprietary structural hydrodynamic model of GRW tankers, validate this model against the results of tanker tests, and report modelling findings.
2. Design, construct and commission a test rig for tests of tankers, including selecting and procuring suitable instrumentation for data gathering.
3. Undertake tests on tankers, including preparing the tankers, assessing the tanker test method and results, and reporting the findings.
4. Determine suitability of tankers for large scale tests and acquire tankers, as appropriate, in accordance with project objectives as specified by DfT.
5. Capture collision and/or deformation data from relevant impacts, for example by laser scanning, to corroborate the modelling and tanker tests, and reconcile any inconsistencies.
6. Engage in peer review activities on the overall DfT research programme.

This report provides an overall summary for the set of reports describing HSL's work on WP1, which are given in Table 1.

Section 2 of this report describes work delivering tasks 4 and 5, the assessment and supply of tankers for the research, which met the objectives:

- Facilitate, as required by DfT, the selection, inspection and procurement of tankers to be used by HSL and other consortium members in the delivery of the project.
- Capture data, including physical samples if needed, from damaged tankers where these data or samples may be beneficial to the project.

If a further tanker's radiography is added, this report will be revised and re-issued.

³ 'Short-term Fitness for Service Assessment of [non-compliant] Road Tankers, TWI (Draft) Report 23437/1/13, September 2013 and 'Project 23437 Contract Amendment: Additional FEA for assessment of [non-compliant] road tankers, TWI (Draft) Report 23437/2/13, October 2013.

Section 3 of this report describes work delivering tasks 2 and 3, the tanker topple test methods and results, which met the objectives:

- Design, construct and commission a test rig for tankers which offers a reliable and repeatable method to provide experimental data for use in both improving the understanding of tanker impact behaviour and validating HSL's Finite Element (FE) modelling.
- Prepare and test tankers to provide experimental data for use in both improving the understanding of tanker impact behaviour and validating HSL's finite element modelling.

Section 4 of this report describes work delivering tasks 1 and 2, modelling to provide load case data for rollover, which met the overall objective:

- Create and validate a structural hydrodynamic model of GRW tankers under rollover conditions.

with more detailed objectives:

- Create an original representative tanker rollover model which includes impact with the ground, realistic fluid motion and rotational velocity, refining an existing HSL structural model of a partial tanker to represent a full GRW tanker so that transverse loading can be modelled.
- Refine the structural hydrodynamic model of the GRW tanker to describe GRW tankers J2580 and J3910 which were topple tested by HSL.
- Validate a suitably refined GRW tanker finite element model against topple test data.
- Apply the validated GRW tanker finite element model to a real-world fuel load representative of real-world conditions and consider the model outputs.

The GRW tankers considered in this research were of “banded” construction - the tanker shell was constructed in short sections, and these were joined using an extrusion band between shell sections. Two circumferential welds joined each extrusion to two shell sections. Bulkheads and baffles were also welded to the extrusion band. In this report the term band is used to mean the constructed extrusion band, including the circumferential welds. The tanker used for the proof of concept test was of stuffed construction - the tanker shell was one single construction, and the bulkheads/baffles were fitted inside and welded to the inner wall of this shell.

Table 1 List of related HSL reports for Work Package 1

ES/14/39/00	Technical Assessment of Petroleum Road Fuel Tankers; Work Package 1 - Full scale testing and associated modelling; Overall Summary THIS REPORT
ES/14/39/07	Technical Assessment of Petroleum Road Fuel Tankers; Work Package 1 - Full scale testing and associated modelling; Assessment and Supply of Tankers
ES/14/39/04	Technical Assessment of Petroleum Road Fuel Tankers; Work Package 1 - Full scale testing and associated modelling; Tanker Topple Test Methods and Results
ES/14/39/05	Technical Assessment of Petroleum Road Fuel Tankers; Work Package 1 - Full scale testing and associated modelling; Modelling to Provide Load Case Data for Rollover – Approach and Initial Development
ES/14/39/06	Technical Assessment of Petroleum Road Fuel Tankers; Work Package 1 - Full scale testing and associated modelling; Modelling to Provide Load Case Data for Rollover - Validation and Application

2 ASSESSMENT AND SUPPLY OF TANKERS

2.1 TANKERS USED IN THE RESEARCH PROGRAMME

2.1.1 GRW tankers

DfT, with HSL support, compiled a list of candidate GRW tankers, based on discussions with and visits to tanker operators and tanker maintenance companies. GRW tankers from this list were selected for use in the research programme, as given in Table 2.

GRW tankers between 2006 and 2012 can be characterised by two extrusion designs and changes in the welding processes for circumferential welds, as follows:

Period A (2006 – approximately middle 2008; jobs J1609 to J2606): Extrusion (between shell sections of tank) with integrated radial web, single sided dish (bulkhead/baffle) to extrusion weld, single wire semi-automated welding process and external tack welds applied during the manufacturing process (along the circumferential seam). J2580 is in this category.

Period B (middle 2008 to middle 2010; jobs J2711 to J3612): Extrusion excluding integrated radial web, double sided dish (bulkhead/baffle) to extrusion fillet weld, single wire semi-automated welding process, manual removal of locating lip prior to welding, internal fillet welds in most bands.

Period C (middle 2010 to 2012; job J3733 onwards, including "FT" job numbers): Extrusion excluding integrated radial web, double sided dish (bulkhead/baffle) to extrusion fillet weld, twin wire semi-automated welding process, manual removal of locating lip prior to welding, internal fillet welds on most bands. J3910 is in this category.

Table 2 GRW tankers considered for the research programme “Technical assessment of petroleum road fuel tankers”

GRW number	Weld type	Year of manufacture	Number of bands	Number of compartments	Research use
J2079	A	2007	10	6	Radiography
J2080	A	2007	10	6	Radiography
J2297	A	2007	10	6	Radiography
J2580	A	2008	8	6	Radiography WP1 Topple test
J3564	B	2009	10	6	Radiography
J3857	C	2010	10	6	Radiography WP2 road test
J3861	C	2010	10	6	Radiography
J3909	C	2011	8	6	Radiography
J3910	C	2011	8	6	Radiography WP1 Topple test
J4171	C	2011	10	6	Radiography
J3217	B	2010	10	1	Damage - rear Laser scan Physical samples for WP2
J3146	B	2009	10	6	Damage - front Laser scan Physical samples for WP2

[One further tanker may be added to this list in a revision of this report.]

2.1.2 Other tankers

The proof of concept test for the topple test method (described in HSL report ES/14/39/04) only required a readily available petroleum road tanker of aluminium construction in roadworthy and loadworthy condition. An 8-compartment 40,000 litre tanker of stuffed, rather than banded, construction met these requirements and was used for the proof of concept test.

2.2 GRW TANKER DESIGN AND CONSTRUCTION

Compartment numbers run from C1 at the front of the tanker. Extrusion bands are labelled from A at the front of the tanker. The number of bands is identified by /8 for an 8-banded tanker and /10 for a 10-banded tanker. The M-*n* labels for bands refer to the naming convention used by a contractor, and run from M-1 at the rear. Where a specific side of a band is referred to, the suffix + has been used to denote the side closer to the front, and the suffix – for the side closer to the rear of the tanker.

The basic configuration of an 8 banded 6 compartment GRW tanker is given in Figure 1. Only compartment C1 contains a baffle. In a 10-banded GRW tanker three compartments - C1, C2 and C4 - contain a baffle as given in Figure 2.

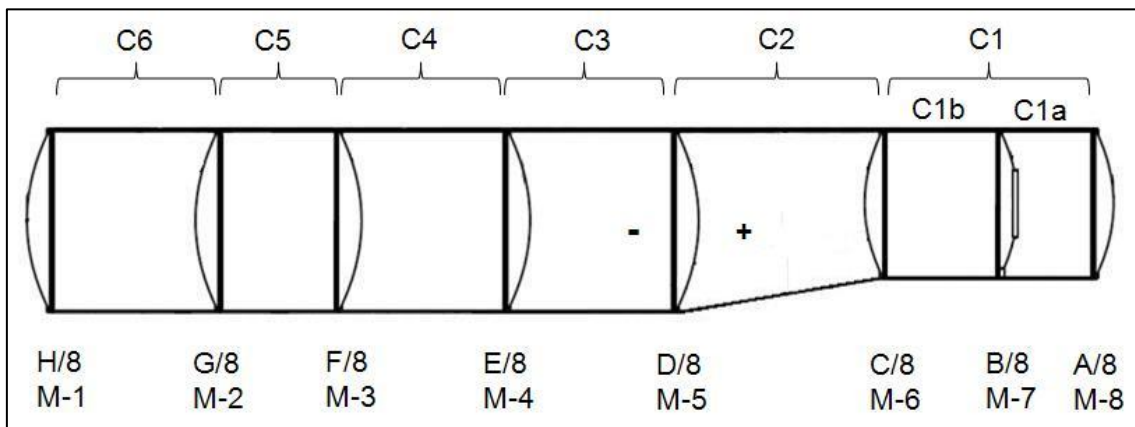


Figure 1 8-banded 6-compartment GRW tanker - bulkheads and baffles
Based on a GRW 44500 L six compartment Tridem tanker, drawing number 085-45-500-03

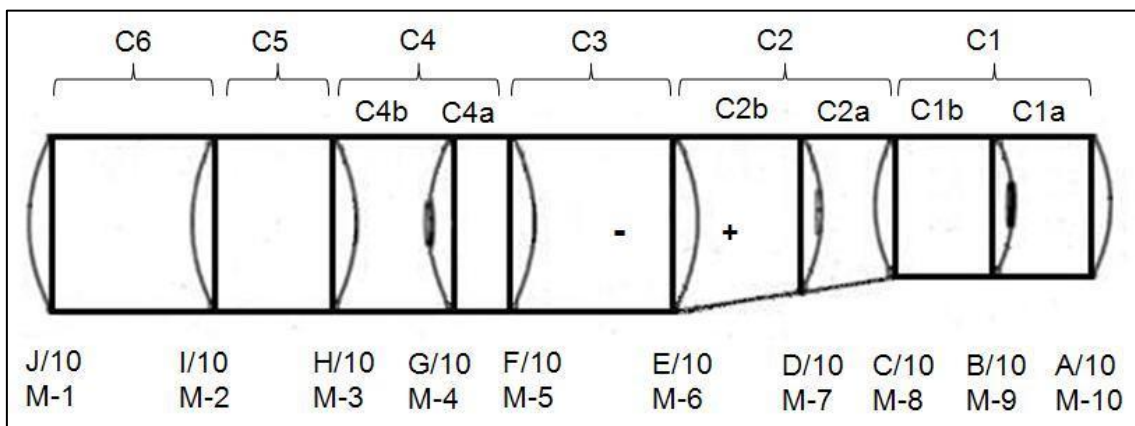


Figure 2 10-banded 6-compartment GRW tanker - bulkheads and baffles
Based on a GRW 44100 L one compartment Tridem tanker, drawing number 085-44-500-05

The 10-banded tanker has a full baffle approximately midway along compartment 2. In the 8-banded tanker, this has been replaced with an internal stiffener ring with two vertical U section struts bolted to it (none shown in Figure 1). In compartment C4 of an 8-banded tanker, the baffle used in the 10-banded tanker has been replaced by a small stiffener along the bottom of the compartment. This stiffener runs across the bottom of the compartment between the locations of the longitudinal support beams. These differences apply to the tankers considered and examined by HSL. They may not be the same for all GRW tankers.

The key design and construction differences between GRW tankers J2580 and J3910 relevant to WP1 were based on construction in GRW weld periods A and C (section 2.1), respectively:

- **Extrusion profile** - GRW tanker J2580 was constructed using a different extrusion profile to that used in GRW tanker J3910.
- **Bulkhead/baffle welding** - On GRW tanker J2580 the extrusion was only welded to the convex side of the bulkhead (or baffle), whereas on GRW tanker J3910 the extrusion was welded to both sides of the bulkhead (or baffle).
- **Fillet welds** - The lengths and positions of the fillet welds with respect to the circumferential welds were different between GRW tankers J2580 and J3910.

2.3 SELECTION OF GRW TANKERS FOR TESTS AND RADIOGRAPHY

2.3.1 Selection criteria

GRW tankers for tests - The primary criteria for GRW tanker selection, for both the topple tests (WP1) and the fatigue data collection activities (WP2) were:

- that the tanker should be representative of 'in-service' UK-based GRW tankers; and
- the condition of the tanker's circumferential welds, based on radiography.

Tankers considered suitable were then further assessed according to other factors including the amount and cost of remedial work needed for the tankers to meet ADR and be roadworthy, their availability and their hire or purchase price.

GRW tankers for radiography - Radiographs were taken (four prior to the project) of the circumferential welds in both 8- and 10-banded GRW tankers covering a range of manufacture dates. This informed the choice of tankers for tests and also provided information on the condition of circumferential welds for a range of GRW tankers.

2.3.2 Selection activities

GRW tankers for tests - The general sequence of activities which, including decision points, varied appropriately for individual tankers, was:

1. Identify GRW tanker and confirm potential price and availability
2. Confirm tanker MOT and roadworthiness and conduct preliminary assessment of ADR condition

decision point

- a. remedial work if needed
3. Transport tanker
4. Radiography of all circumferential welds
 - a. assess radiography

decision point

5. Transport tanker for inspection or return to owner
6. Full ADR inspection of tanker
 - a. other loadworthiness inspection

decision point

- b. remedial work if needed

7. Transport tanker for further inspection or return to owner
8. Other (optional) pre-test inspections of tanker
 - a. partial inspection corresponding to some aspects of full periodic ADR inspection
 - b. second radiography of some or all circumferential welds
 - c. pre-test survey of tanker, for example internal visual examination of welds
9. Optional pre-test work preparing tanker for test by third party
10. Transport tanker to test location

GRW tankers for radiography - The sequence for activities followed the same general process, at least as far as step 5.

2.4 RADIOGRAPHY OF GRW TANKERS

Ten⁴ GRW tankers have been fully radiographed, covering all the bands. These tankers are listed in Table 2. GRW tanker J2580 has been partially radiographed a second time, and GRW tanker J3910 has been fully radiographed a second time, with second radiography conducted by a different contractor to the first.

2.4.1 Radiographic examination

Both contractors used the single wall, single image (SWSI) approach. Contractor 1 used the SWSI Source outside the tanker and the image plate (film) inside the tanker, while contractor 2 used the reverse with the SWSI Source inside the tanker and the image plate (film) outside the tanker. All assessment was to EN ISO 10042: 2005 [1] Quality Level 'C'. Curvature of the bulkheads/baffles restricted internal access to the concave side of the baffle plates.

Contractor 1 took radiographs of the circumferential welds for all the bands on both the offside and the nearside of all the tankers radiographed, from the lowest accessible position on the band to the comb. Radiographs in the comb area were also taken for some tankers. Contractor 2 took radiographs of GRW tanker J2580 circumferential welds on the offside only for the rear three bands, F/8 (M-3), G/8 (M-2) and H/8 (M-1), from the lowest accessible position on the band to the comb. Contractor 2 also radiographed the circumferential welds for all the bands of GRW tanker J3910 on both offside and nearside, from the lowest accessible position on the band to the comb.

Bands were divided into shorter sections for the individual radiograph exposures which combined to form the overall radiography of the band. In general these sections were 35 cm long for contractor 1 and 30 cm long for contractor 2, with shorter lengths where necessary. (Distances were over the curved surface of the tanker.)

2.4.2 Starting positions of radiographs on the tankers

The starting positions of radiographs on the tankers were similar for 8- and 10-banded GRW tankers with respect to the support ribs at the bands. HSL have only inspected 8-banded tankers closely. Figure 3 illustrates the radiograph starting positions for the offside of 8-banded tankers; positions on the nearside and offside were similar. Radiographs of bands D/8 to H/8 (M-5 to M-1) started just above the top of the hose tray which runs along the tanker. The top of this hose tray was higher than the top of the support ribs which sit on the bands, as illustrated in Figure 4 which shows the nearside of GRW tanker J2580 before delivery to HSL. Radiographs of bands A/8 to C/8 (M-8 to M-6) started above the support ribs which sit on the bands.

⁴ one further tanker may be added to the list

For 10-banded GRW tankers, starting positions for radiographs of bands E/10 to J/10 (M-6 to M-1) were just above the top of the hose tray which runs along the tanker. The starting positions for bands A/10 to D/10 (M-10 to M-7) were above the support ribs which sit on the bands.

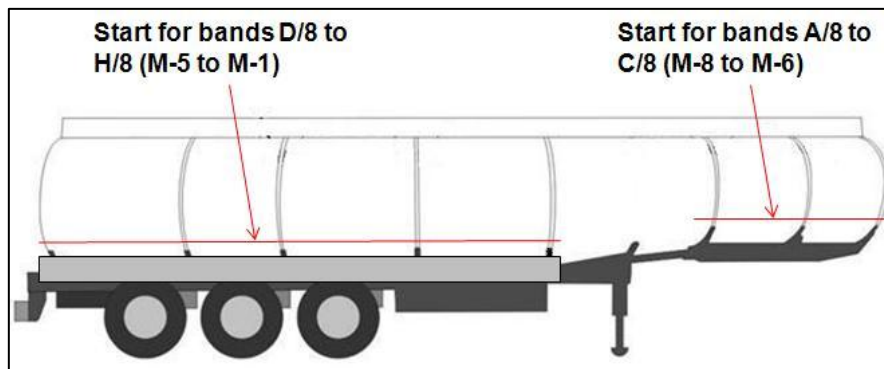


Figure 3 Schematic of radiograph starting positions for GRW 8-banded tanker
Support ribs are shown above the top of the hose tray to make their position clear



Figure 4 Nearside of GRW tanker J2580 with hose tray
Radiography of bands D/8 to H/8 started just above the top of the hose tray

2.4.3 Radiography reports

The radiography reports noted where the following features were found on the individual radiograph sections, and over what lengths:

- lack of fusion (LOF);
- intermittent lack of fusion;
- linear porosity;
- porosity;
- isolated pores;
- lack of penetration (LOP); and
- inclusions.

An overall acceptance or rejection for each individual radiograph section was given in the radiography reports, together with summaries of the number of defects and percentage length of defects in terms of total radiographed length in each band. Contractor 1 also provided photos of the tanker and the radiograph starting positions in the radiography reports.

2.5 DAMAGED GRW TANKERS

Two damaged GRW tankers, J3217 and J3146, were used to provide information for the research programme.

2.5.1 Damaged tanker J3217 - rear impact damage

GRW tanker J3217 was damaged at the rear offside by an impact from behind (Figure 5). It was laser scanned by HSL to provide dimensional information on the whole tanker, including the damage. Figure 6 is an image from the laser scan data. Physical samples of the damaged areas were taken for use in WP2.



DfT IMG9444

Figure 5 Damage to the rear of GRW tanker J3217



Figure 6 Laser scan image of the rear GRW tanker J3217

2.5.2 Damaged tanker J3146 - Front impact damage

GRW tanker J3146 was damaged at the front offside corner, at band A/8, by an impact. While awaiting repair, GRW tanker J3146 was laser scanned by HSL to provide dimensional information on the whole tanker, including the damage. Physical samples from the damaged areas were taken for use in WP2 when the repair was made.

3 TANKER TOPPLE TEST METHODS AND RESULTS

3.1 METHODS

3.1.1 Topple test approach

After considering various approaches, including ADR clause 6.5.6.11 [2], and discussing the proposed test method with the research consortium, HSL developed a topple test to roll over a suitably instrumented tanker in a controlled and repeatable way. This was a uniform longitudinal dynamic impact of the tanker side with the surface of a prepared test pad, resulting from the lateral rotation of the tanker around the axis formed by the outer edge of the tanker's road wheels. The test principle was to tilt a tanker, quasi-statically, to the point where its centre of gravity was above the axis of rotation, as illustrated in Figure 7. Once in this position, the stability of the tanker was sufficiently compromised such that only a small additional impetus was required to induce the tanker to topple. The tanker was filled with water to represent the fuel load: petroleum, diesel or fuel oil was not practical for environmental and safety reasons.

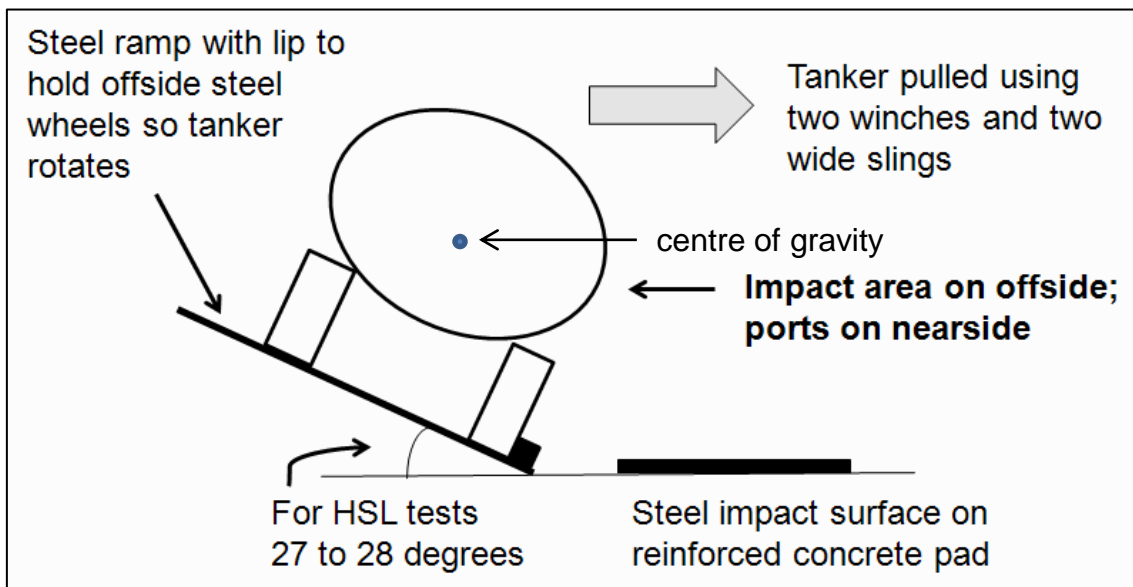


Figure 7 The key features of the HSL tanker topple test

Information on the tanker's dimensions, geometry and centre of gravity was used to calculate the approximate angle at which the tanker would become unstable (above 28 degrees). The static and dynamic loads involved were calculated and used in the design of ramps which were manufactured to provide an initial tilt angle, at several degrees less than the angle required for topple. These ramps were secured to a 25 m x 40 m concrete test pad. Plate steel secured to the landing pad provided a more robust and repeatable impact area.

The empty tanker was lifted onto the ramps so the sides of the wheels were parallel to the bottom edge of the ramp. To eliminate the risk of the offside tyres coming off the wheel rims during the test, and to avoid variability from uncontrolled shear movement in these tyres during the topple, the offside wheels were replaced with dimensionally similar rectangular steel supports ('steel wheels'). The offside steel wheels were close to the bottom of the ramps, and the nearside wheels were close to the top of the ramps. Impact was on the offside of the tanker to avoid damage to the filling ports on the nearside of the tanker. Once in position on the ramps, and prepared for test, the tanker was filled with the required volume of water evenly distributed

across all the individual compartments. The tanker was then toppled sideways, pivoting around the outer edge of its offside wheels.

The tanker was not tested with a tractor unit to avoid uncontrolled variations between tests caused by tractor unit rotation and possible failure of the kingpin due to unconventional loading. Instead, a steel frame, known as the 5th wheel assembly, was fitted to the tanker at the front (kingpin plate) to give the support normally provided by the tractor and to keep the tanker at the desired coupling height for the test. The tanker's suspension was blocked and held rigid to remove sources of uncontrolled variation, such as changes in the ride height, and to keep the tank position fixed relative to the suspension during the topple. The static and dynamic loads for all the tanker modification components were calculated and used in their design.

The tanker was rotated into the topple position using two parallel winching systems (the winches were two horizontally-positioned chain hoists) with wide slings to spread the load and prevent high stress levels on the tanker body and comb when the winch forces were applied to the slings. Each wide sling was attached to the tanker on the nearside and passed around the top of the tanker body: one sling at the 5th wheel near the front of the tanker and the other sling at the rear and middle axles near the rear of the tanker. Each winching system included a chain hoist and load cell and was anchored to the concrete pad.

Rotating the tanker into the topple position was controlled by ensuring the load on each winch line was similar, giving an 'even pull'. A 'Winch Master' controlled the operation by monitoring the load on each line and giving orders to the 'Winch Operators' to ensure that the loads on each line remained similar. As the winches began to take the weight of the tanker, the tanker rotated and pivoted around the offside steel wheels and the offside of the 5th wheel assembly. When the point of instability was reached, the winching lines slackened and the tanker toppled onto its side under the influence of gravity.

3.1.2 Tankers tested

Three tankers were tested. First, a proof of concept test was conducted on a 'guinea pig' aluminium petroleum road tanker, which met the needs for the proof of concept test rather than the full tanker specification. The aim of this test was to establish that the basic test method and data logging system were sound, so minimal test instrumentation was used on the tanker, with the full data logging system operating. All the key features of the preparation and topple test, including tanker recovery, were conducted, so that improvements or modifications to the test method could be considered.

Second and third, respectively, GRW tankers J2580 (8-banded 6-compartment, 2008) and J3910 (8-banded 6-compartment, 2011) were tested with full test instrumentation. The configuration of these tankers is given in Figure 1 (section 2), together with compartment and band numbering.

3.1.3 Tanker preparation

All tankers were prepared for test by:

- removing any items on the tanker which were not integral to the tank and suspension and which might adversely affect the impact, for example by damaging the tanker shell;
- removing or sealing any items on the tanker which might contain fuel, hydraulic oil or other environmentally harmful materials;
- replacing the offside wheels with steel wheels;
- adding the 5th wheel support frame at the kingpin plate; and
- blocking the tanker's suspension to hold it rigid.

3.1.4 Tanker instrumentation

The full data gathering instrumentation for GRW tankers J2580 and J3910 comprised strain gauges, pressure transducers and accelerometers. These provided data for finite element model validation and characterising general impact behaviour. Arrays of strain gauges and pressure transducers were mounted in compartments C1b (rear half of front compartment) and C4 (third compartment from the rear) as follows:

- seven pressure transducers in each compartment, located at the midpoint of the compartment close to the inner tanker wall, radiating circumferentially top to bottom on the offside (impact side), the centre being at the estimated point of impact; and
- twelve strain gauges for each compartment, as strain gauge pairs in matching positions on the inside and the outside of the offside tanker shell. For GRW tankers J2580 and J3910 one location was near the rear bulkhead weld measuring longitudinal strain and one location was at the midpoint of the compartment measuring both longitudinal and hoop strain. For GRW tanker J3910 only, a further location was near the front bulkhead weld measuring longitudinal strain. All strain gauges were mounted at the same level (around the hose tray line in Figure 4), with this level chosen so that they were below the bottom of the impact zone.

Accelerometer blocks were located at the centre point on the outside of both the front and rear bulkheads.

The locations for instrumentation used on GRW tankers J2580 and J3910 are given in Figure 8.

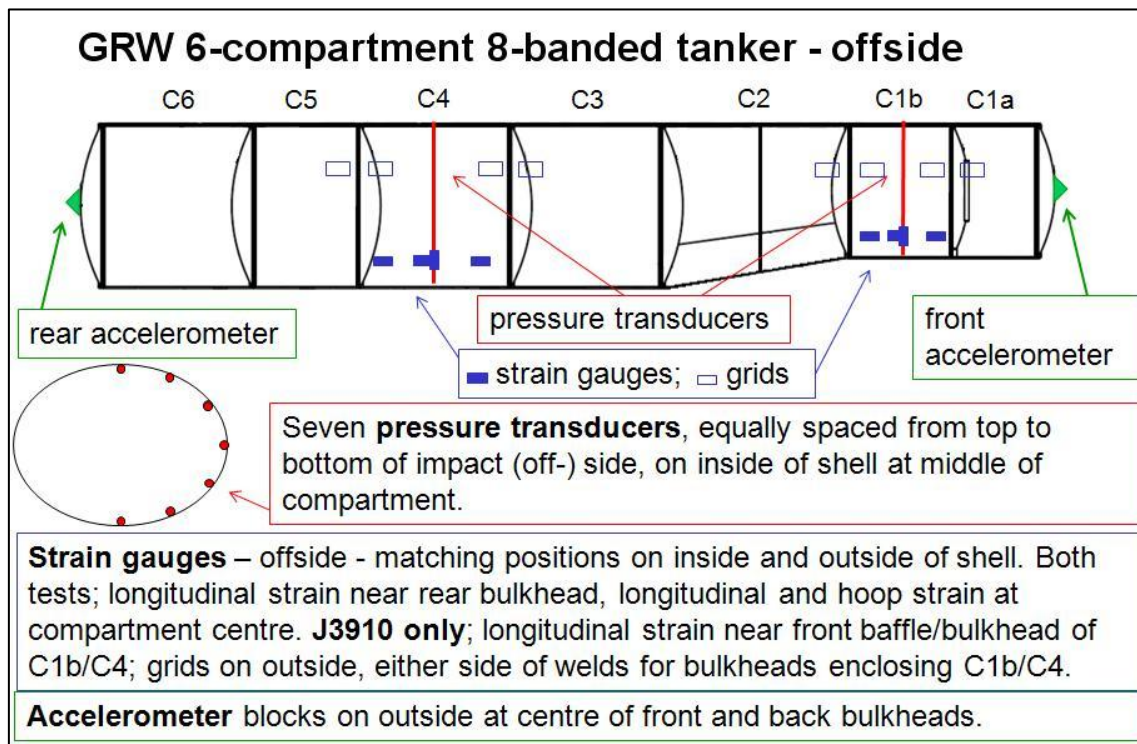


Figure 8 Location of instrumentation on GRW tankers J2580 and J3910

On GRW tankers J2580 and J3910 cables from instrumentation located inside a compartment passed out of the compartment through a specially designed baffle. This cabling then led to connectors or junction boxes which linked the tanker instrumentation to the main wiring loom connected to the data loggers. Cables from instrumentation on the outside of the tanker were also brought to these junction boxes.

Two independent data loggers were used, with each logger specific to one of compartments C1b and C4. During the topple test these loggers were synchronised with the high speed video and set to acquire data at a rate of 50,000 samples per second (50 ks/s), or one recording every 0.02 millisecond. Slower data acquisition rates were used during some preparation activities and during filling before the test.

The proof of concept test tanker was fitted with accelerometers on the outside of the front bulkhead, but no other instrumentation. The full data logging system was run during this test.

3.1.5 Pre-test inspection of tankers

The proof of concept tanker was laser scanned after preparation but before lifting onto the ramps, after topple (on its side) and after recovery upright onto its wheels. GRW tankers J2580 and J3910 were laser scanned 'as received', after lifting onto the ramps, after topple (on their sides) and after recovery (upright, on their wheels). This provided general dimensional data and allowed confirmation of:

- any changes caused by HSL preparation of the tanker; and
- any changes to the tanker dimensions and shape after the impact.

The internal circumferential welds in GRW tanker J2580 were visually inspected during preparation, and the locations of fillet welds between the extrusion band and the shell were noted. A fuller survey of the internal circumferential welds in GRW tanker J3910 was made, including the locations of misalignments, fillet welds between the extrusion band and the shell and other features. The external weld caps on the circumferential welds in GRW tanker J3910 were surveyed by laser scan to provide dimensional data on cap height and width, cap spacing and misalignment for the WP2 detailed ECA.

Grids, comprising a 5 by 5 array of circles, were applied to the outside of GRW tanker J3910 above the likely impact zone, either side of the bulkhead and baffle welds which enclose compartments C1b and C4. These grids were intended to provide indication of the deformation close to the welds in the compartments with strain gauges for WP2 activities.

Once preparation of GRW tankers J2580 and J3910, including fitting all instrumentation, was complete, their manway lids were refitted and a pneumatic pressure test was conducted to confirm that the tankers remained fully sealed and loadworthy, with full internal and external integrity.

3.1.6 Tanker filling

Immediately before test, tankers were filled with water using a calibrated water meter. The proof of concept tanker was filled to about 90% by volume, the nearest to the volume that would be used for a fuel load (95% full, 5% ullage) that could be achieved when the tanker was inclined on the ramps. This gave a volume of 37,990 litres or a mass of 37,990 kg for water density 1,000 kg/m³. Although this was above the tanker's rated maximum load, it provided a severe test of the mechanical integrity of the test system.

For GRW tankers J2580 and J3910, it was agreed by the research consortium to fill the tankers to their maximum rated load mass (31,380 kg), which was below their rated volume for fuel. Both GRW tankers J2580 and J3910 were filled with 31,376 litres of water, with each compartment filled to about 70% of its maximum capacity.

3.1.7 Photography and video

The proof of concept test was recorded using nine video cameras, ranging from standard speed (25 frames per second) to high speed (1000 frames per second). The tests of GRW tankers J2580 and J3910 were recorded using thirteen video cameras ranging from standard speed (25 frames per second) to high speed (1000 frames per second), plus hi-quality stills photos and time-lapse of the preparation at the pad, tests and after-test at the pad activity. Frames from the high speed video were analysed to obtain accurate measurements of acceleration and impact velocity at the front and rear of the tanker.

3.1.8 After-test activity

Immediately after impact, visual examination was used to identify leaks and other impact features. The tanker was then emptied before being lifted back to be upright (on its wheels). After recovery there was further visual examination. For GRW tankers J2580 and J3910, a pressure test was then conducted to ascertain the internal integrity of the compartments and bulkheads. Physical samples were taken from both tankers for use in WP2.

3.2 RESULTS

3.2.1 Test rig and method

The proof of concept test was successful, with no major problems found in the topple test rig or test method. Some minor improvements in the exact sequence and detail of the test were noted and implemented during the GRW tanker tests. These tests on the GRW tankers were also successful, with no problems from the test rig or test method.

3.2.2 Instrumentation and data gathering

In the proof of concept test, tri-axial accelerometer data for z-axis (longitudinal) acceleration contributed little value, and this axis was not measured in subsequent tests. High frequency accelerometer components, from vibration (ringing) in the tanker body after impact, were undesirably high. A thin resilient strip was placed between the accelerometer and tanker body for measurements on the GRW tankers to reduce this. In the two GRW tests, there was good agreement between the accelerometer data and acceleration values obtained by analysing the high speed video.

All 44 channels of instrumentation provided valid data for GRW tanker J2580. For GRW tanker J3910, all but three channels of instrumentation provided valid data; signals from the corresponding three internal strain gauges were lost when the gauges came into contact with the water during filling. Although the signals from these gauges re-appeared during the impact, with their trend after this being similar to comparable gauges, there was an offset in their values and data from these three gauges cannot reliably be compared with the data from the finite element model.

3.2.3 Impact behaviour

The overall impact duration was a few seconds for all the tests, with most deformation occurring in the first 100 ms. Using the high speed video:

- The proof of concept tanker was found to have impacted reasonably uniformly along its length, with front and rear hitting the ground within a few milliseconds of each other. The impact speed at the rear of the tanker was 4.25 m/s (around 2 rad/s) - due to the nature of the test, impact speed was not measured at the front of the tanker.
- GRW tanker J2580 impacted with speeds of 4.50 m/s (1.82 rad/s) at the front and 4.10 m/s (1.86 rad/s) at the rear of the tanker, and the rear hitting the ground first, less than 1 ms before front of the tanker.

- GRW tanker J3910 impacted with speeds of 4.55 m/s (1.84 rad/s) at the front and 4.25 m/s (1.93 rad/s) at the rear of the tanker, and the rear hitting the ground first, less than 7 ms before front of the tanker.

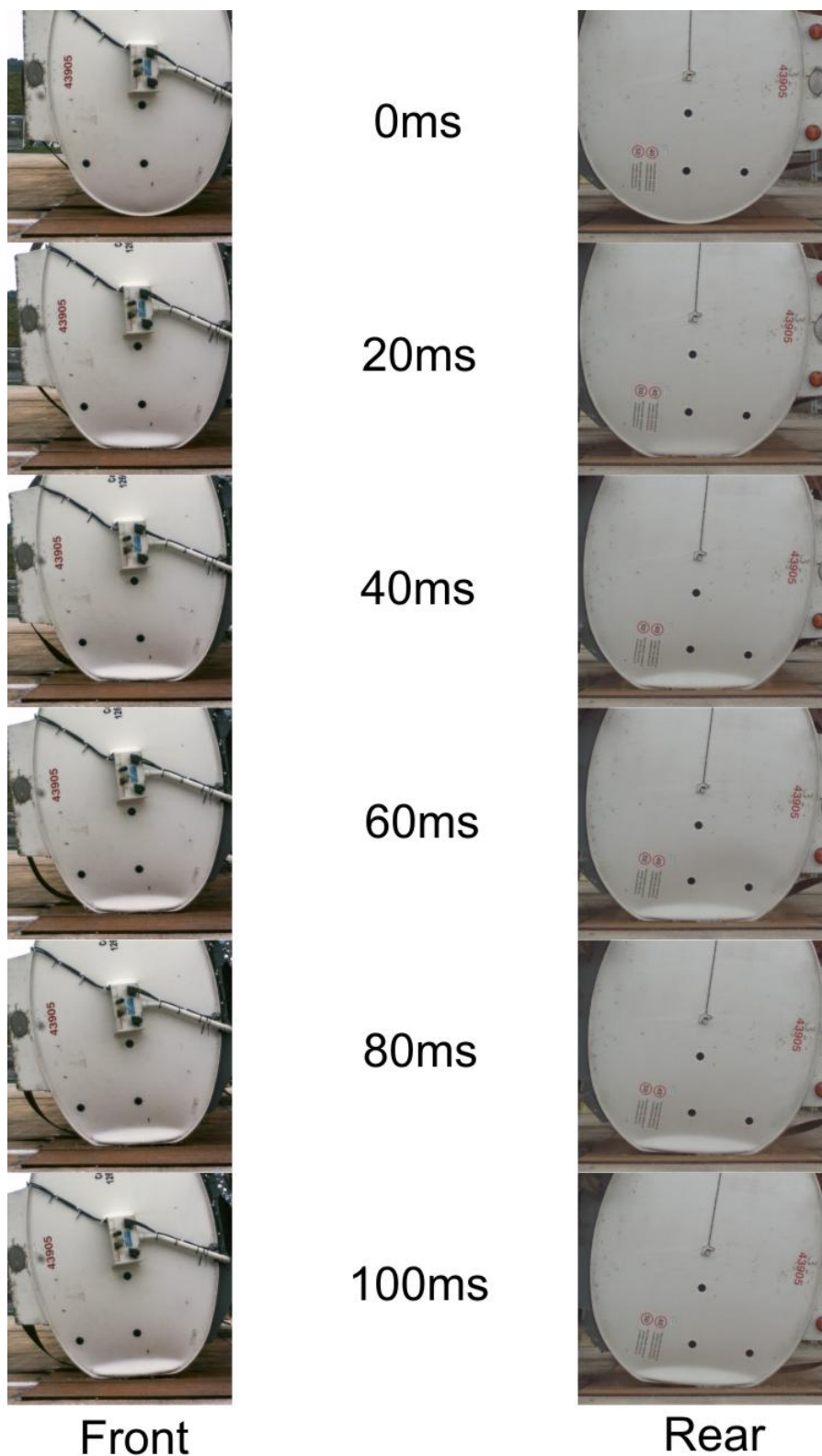
These impact velocities lie within the range of those for rollover in real accidents, where impact velocities of between 100 to 150 degrees/s, which correspond to 1.75 to 2.62 rad/s, have been reported [3].

The behaviour after first impact was different for all three tankers:

- The proof of concept tanker continued to roll forward, away from the ramps, until at 40 to 50 degrees the comb along the top of the tanker hit the ground, after which the tanker rolled back before coming to rest on its side (at 0 degrees).
- GRW tanker J2580 slid forward and also rolled forward 10 to 15 degrees, then slid and rolled back before coming to rest on its side (at 0 degrees).
- GRW tanker J3910 slid forward and also rolled forward 10 to 15 degrees, then rolled back but hardly slid back before coming to rest on its side (at 0 degrees).

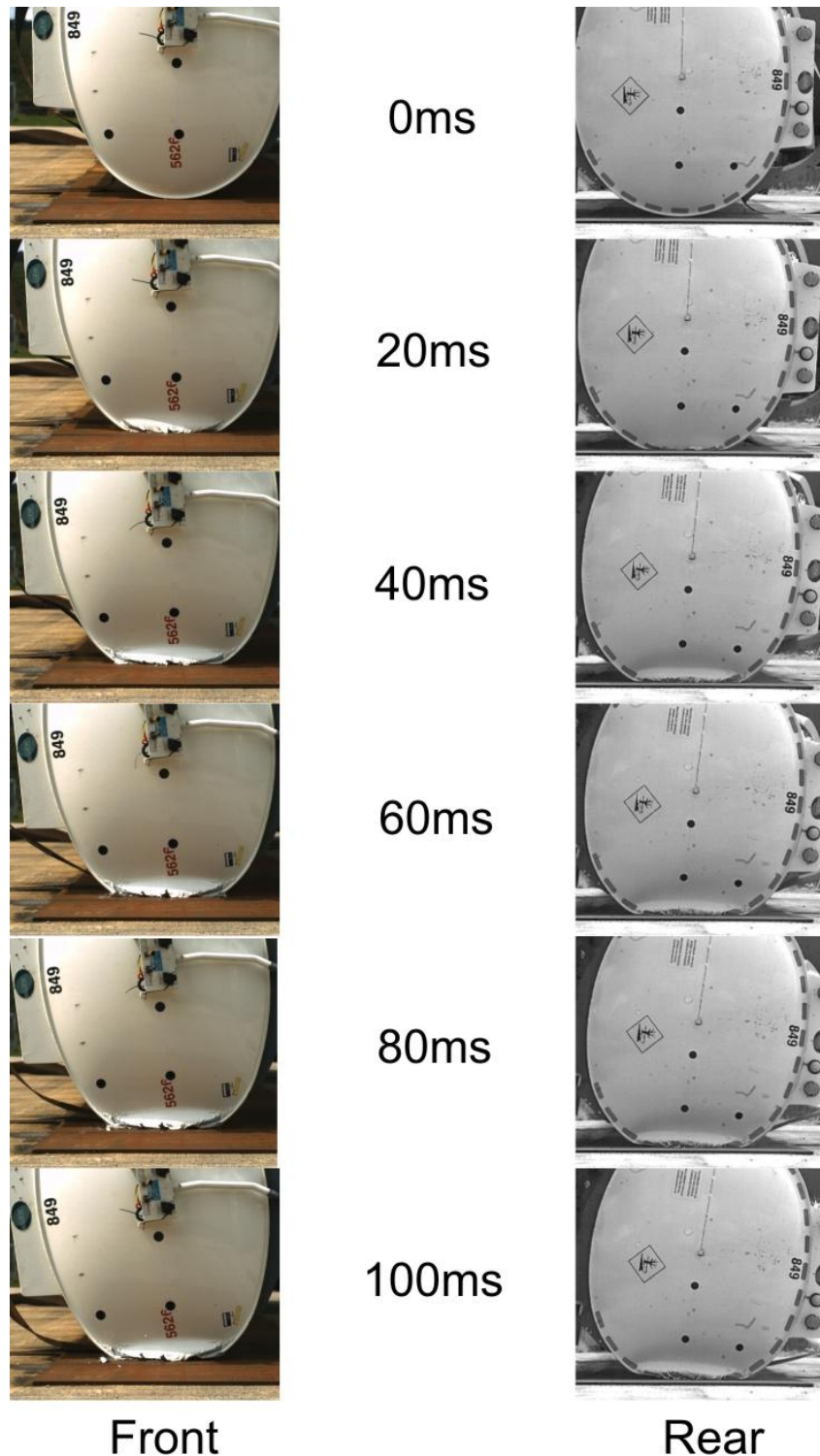
It is likely that the higher load mass for the proof of concept tanker was the significant factor in the difference between its behaviour and that of the GRW tankers.

Six images for each end of the tanker, in 20 ms steps from the moment of impact to 100 ms later, are given in Figures 9 and 10 for GRW tankers J2580 and J3910, respectively.



Video Sequence For J2580

Figure 9 High speed video images during impact – GRW tanker J2580



Video Sequence For J3910

Figure 10 High speed video images during impact – GRW tanker J3910

3.2.4 Impact and deformation data

The pressure data in both compartments were similar for GRW tankers J2580 and J3910 (Figure 11). Short duration pressure peaks between 2 and 7.7 bar (28.4 and 110 psi) were observed during the first 20 to 30 ms of the impact; these were above the 2 bar (28.4 psi) used in previous rollover modelling by Bysh and Dorn, 1996 [4]. However, between around 20 and 40 ms after impact the pressures were around 2 bar, and after this the pressures reduced further.

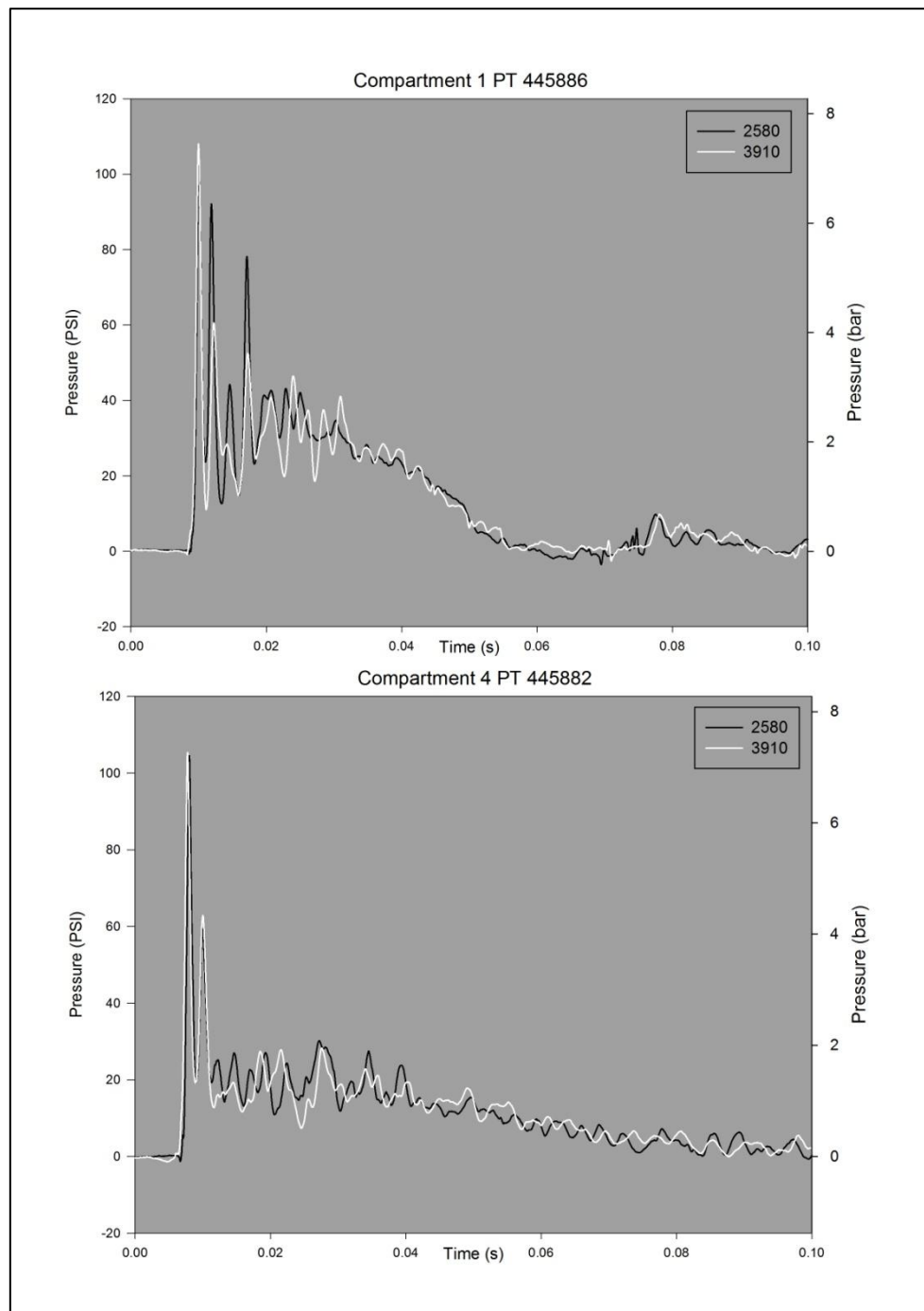


Figure 11 Comparison - pressure measured at the centre of the impact area.

The strain data in both compartments were similar for GRW tankers J2580 and J3910. Strains at the centres of the compartments were reasonably consistent between the two tankers, with more variation in the hoop strains than in the longitudinal strains. During impact, for both GRW tankers, high speed video captured free travelling flexural waves propagating away from the impact line around the circumference of the tanker. Such waves should result in more pronounced ripples in the circumferential strain than the longitudinal strain at the centre of the compartment, as was found to be the case for both GRW tankers. Strains near the welds were higher than those at the compartment centre, with some yielding and plastic deformation observed in the strain behaviour near the welds, for example location Wb in compartment C4 (Figure 12).

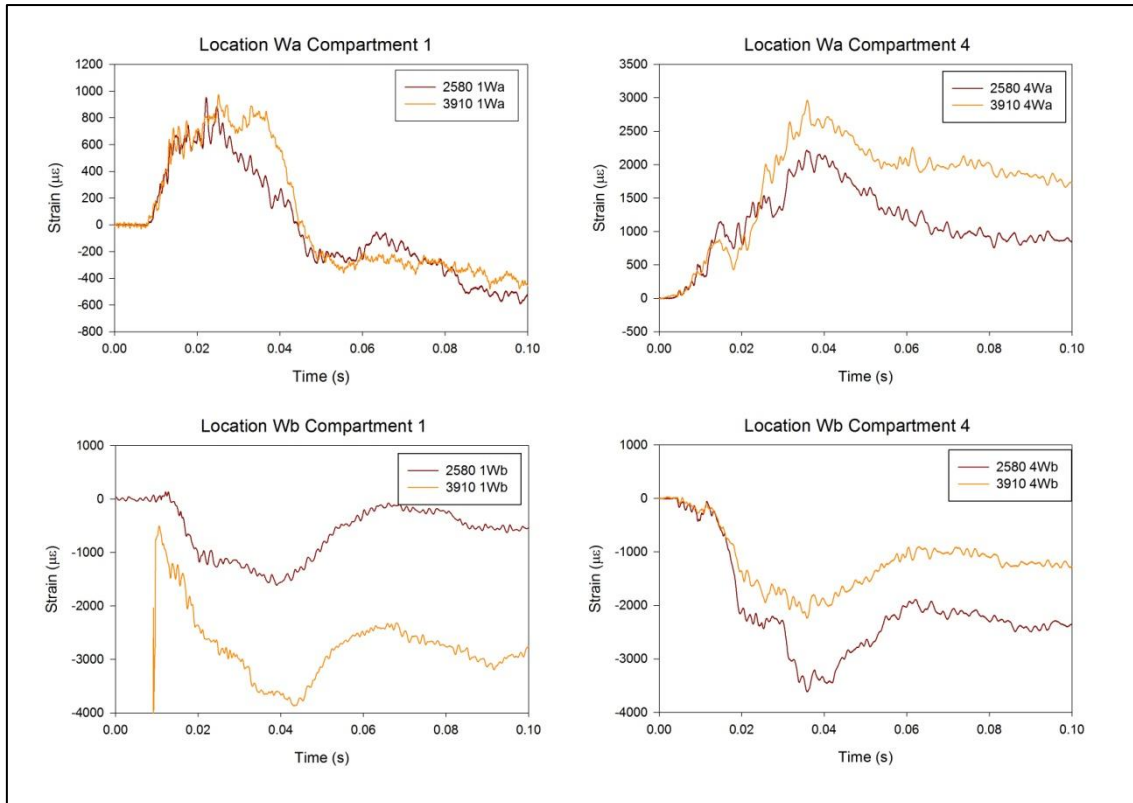


Figure 12 Comparison - longitudinal strain near rear bulkhead in C1b and C4

The J3910 data for Wb in compartment 1b is from one of the strain gauges which did not function correctly. The trend is shown for indication - the magnitude of the values is unreliable.

After the test, the offside (impact side) of all the tankers had a similar deformation shape with the impact area flattened - Figure 13 illustrates the damage to GRW tanker J3910. The deformation profile was similar along the length of the GRW tankers, with the level of deformation increasing from front to rear of the GRW tankers. The deformation data, both as a reduction in tanker diameter and as the length of the flattened impact chord, were similar for GRW tankers J2580 and J3910. Comparison of laser scan images taken before and after the tests showed that the impact had caused permanent reduction in tanker diameter of approximately 100 mm at the rear of the proof of concept tanker; of approximately 100 mm at the rear and 82 mm at the front of GRW tanker J2580; and of approximately 107 mm at the rear and 82 mm at the front of GRW tanker J3910.



VPS 1407047_006 - picture enhanced to make damage clearer

Figure 13 GRW tanker J3910 - impact damage viewed from front

3.2.5 Impact damage

Proof of concept tanker. During impact, water was expelled from the tanker through the manway pressure relief valves, and some valves continued to leak after the test. As these valves had not been checked and correctly resealed, if required, before the test, this was not surprising. Immediately after the test there was a small leak at the top of the impact area at the front of the tanker where the front dish, front bulkhead and front side wall were significantly buckled. When the tanker manways were opened, little water remained because the welds connecting all the internal bulkheads to the shell of the tanker had failed near the impact area so that all compartments had lost their internal integrity and most of the water which had not leaked from the valves had leaked away through the rupture at the front of the tanker.

GRW J2580. During impact, a small amount of water was lost through the pressure relief valves; much less than was observed for the proof of concept tanker. Immediately after the test, the only visible leak from the tanker was between the rear bulkhead and extrusion band at the top of the impact area. Subsequent visual inspection found a rupture within the weld between the rear bulkhead and extrusion band at the top of the impact area (Figure 14). Folding of the rear bulkhead over the weld along most of the impact area prevented assessment of the extent of this rupture across the impact area. However, there was no visible damage at the bottom of the impact area where the rear bulkhead was not folded over the weld. Before the water was pumped out of each compartment, no obvious lowering of the water level in the adjacent compartments was observed; so it was unclear if there had been any breaches between compartments. Once the tanker had been lifted back onto its wheels, pneumatic pressure tests found that all compartments had lost their internal integrity. On this tanker the bulkheads were welded to the extrusion bands on one side, the convex side of the bulkhead curvature, and not to both sides of the extruded band. The convex side of the rear bulkhead was the outside.

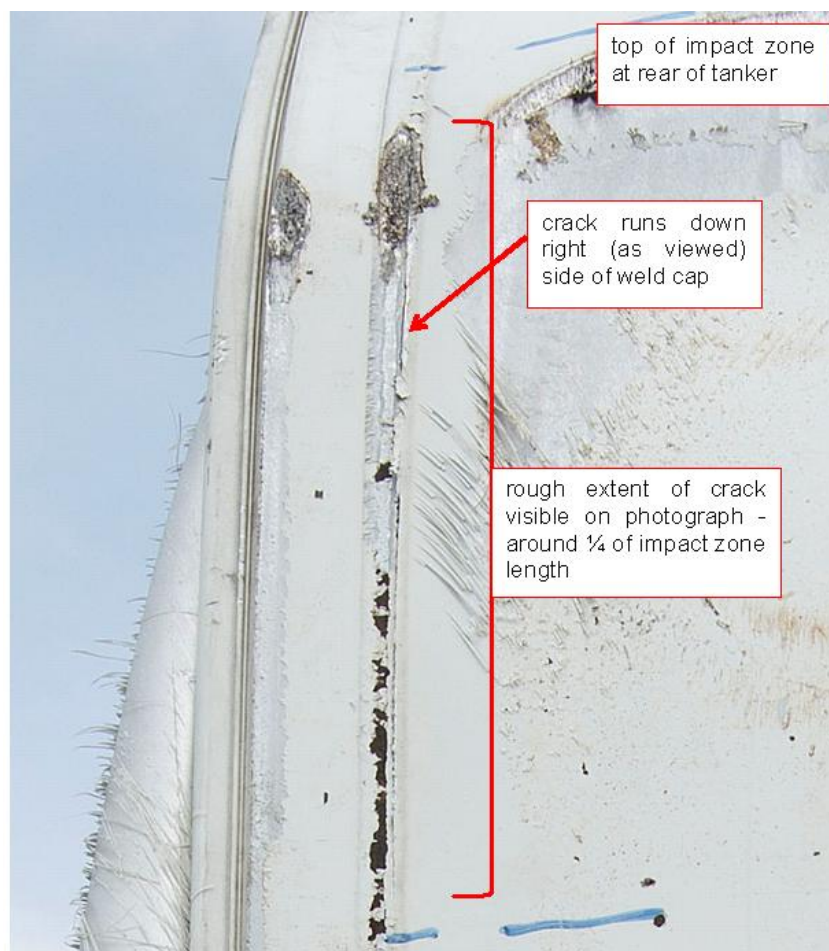
HSL supplied TWI with a sample of the impact zone from the off-side rear (band H/8) and a sample of the equivalent portion on the near-side from GRW tanker J2580 for post-mortem assessment under WP2. During post-mortem examination, TWI observed an apparent through-wall crack along the circumferential weld at the top of the impact zone. This apparent crack can

be seen in Figure 15, which is taken from close examination of an HSL photograph of the tanker after being lifted back onto its wheels.



VPS 1408025_017

Figure 14 GRW tanker J2580 – rupture in the weld at top of impact zone



VPS 140523_16

Figure 15 GRW tanker J2580 – apparent through-wall crack along the circumferential weld at the top of the impact zone at the rear (band H/8)

GRW J3910. During impact, a similar amount of water was lost through the pressure relief valves as for GRW J2580. Immediately after the test, the only visible leak from the tanker was between the front bulkhead and the extrusion band at the top of the impact area. Subsequent visual inspection found a rupture in the toe of the weld between the front bulkhead and the extrusion band at the top of the impact area (Figure 16). Folding of the front bulkhead over the weld along most of the impact area prevented assessment of the extent of this rupture across the impact area. However, there was also a crack in the toe of the weld at the bottom of the impact area where the front bulkhead was not folded over the weld (Figure 17). Before the water was pumped out of each compartment, compartment 1 had emptied through the leak at the front bulkhead, and compartment 2 had started to empty. This suggested a leak at the bulkhead between compartments 1 and 2. Similarly, when compartment 4 was emptied, the water level reduced in compartment 5, suggesting a leak at the bulkhead between compartments 4 and 5. Once the tanker had been lifted back onto its wheels, pneumatic pressure tests confirmed that internal integrity had been lost between compartments 1 and 2 and between compartments 4 and 5, while the other bulkheads and compartments had maintained their internal integrity. On this tanker the bulkheads were welded to the extrusion bands on both sides of the bulkhead.

HSL supplied TWI with a sample of the impact zone from the off-side front (band A/8) from GRW tanker J3910 for post-mortem assessment under WP2.



VPS 1408025_025

Figure 16 GRW tanker J3910 – rupture at toe of weld at top of impact zone



VPS 1408025_006

Figure 17 GRW tanker J3910 – crack at toe of weld at bottom of impact zone

GRW have indicated that the damage around the joints between the extrusion band and the bulkhead/baffles is consistent with that seen in real-world rollovers.

3.3 TEST UNIFORMITY AND USE OF TEST DATA FOR HSL'S FINITE ELEMENT MODEL

Overall, the test method met the objective of providing a reliable and repeatable method very successfully. The consistent impact behaviour and instrumentation data for the GRW tankers J2580 and J3910 was evidence of the test method's repeatability.

Section 4 (and HSL report ES/14/39/06) describes how the test data from GRW tankers J2580 and J3910 was used to refine and validate HSL's finite element model of tanker rollover.

4 MODELLING TO PROVIDE LOAD CASE DATA FOR ROLLOVER

A suitable initial finite element (FE) model for GRW tanker rollover based on HSL's topple test was created. This model has been refined and validated against experimental data from HSL's topple tests of GRW tankers, and then used to consider real-world fuel loads. The modelling software used was ANSYS Autodyn version 15. A list of models used is included in Table 3.

Table 3 List of models created

Model	Impact Velocity rad/s	Extrusion profile used	Fillet weld locations	Liquid	Notes
J2580 2.0	2.0	J2580	As GRW drawing	Water	
J2580 1.89	1.89	J2580	As GRW drawing	Water	
J3910 Original	2.0	J3910	Based on J3910 tanker	Water	
J3910 Modified	1.89	J3910	Based on J3910 tanker	Water	Some non-structural members thickened to increase mass. Mesh refined.
Fuel Oil 2.0	2.0	J3910	Based on J3910 tanker	Fuel Oil	Based on J3910 Original model. Compartment 3 empty.
Fuel Oil 2.6	2.6	J3910	Based on J3910 tanker	Fuel Oil	Based on J3910 Original model. Compartment 3 empty.
Petrol	2.0	J3910	Based on J3910 tanker	Petrol	All compartments full

4.1 INITIAL DEVELOPMENT OF THE TANKER ROLLOVER MODEL

The majority of the mass in a fuel tanker with a full load consists of the fuel load (approximately 30 tonnes of fuel and 5 tonnes for the tanker body). Therefore, an appropriate representation of the fuel is necessary to accurately model the event. After consideration of alternative approaches, the Euler/Lagrange fluid structure interaction approach was chosen for the analysis of the tanker topple event. This approach allows the detailed geometry of the tanker to be represented using shell elements and the liquid in the tanker to be modelled.

The impact of the tanker with the ground is a highly dynamic event, with an impact velocity around 4 m/s, and is likely to result in large deformations and high levels of strain. In terms of dynamic analysis, this is relatively slow (compared to ballistic events, for example) but it is still

fast enough to be suitable for an explicit analysis. The duration of the main impact which causes the majority of the deformation and stress in the tanker was approximately 100 ms.

The empty space in the tanker's compartments was modelled as a void, as opposed to assuming air or air/fuel vapour, as this approach was much more efficient in terms of solution time. It also prevented the build-up of pressures in the compartment due to the reduction in volume caused by crushing, as in reality this build-up would be prevented by the tanker's pressure relief valves.

As this model does not consider the detailed behaviour of the welds at the extrusion bands, a mesh size of between 10 mm and 20 mm was found to be appropriate for the sections of the tanker subject to the largest deformations, and very little difference in deformation values was observed with further refinement. However, when data from this model was compared to topple test data the mesh size was refined in some key locations.

GRW tankers J2580 and J3910 used different extrusion designs in the construction of the bands which join the sections of the tanker together, so geometries for both designs were created for the model of the extrusion band. These tankers also included fillet welds in different positions on their circumferential welds. Geometries for the extrusion band with and without fillet welds were created for use where appropriate.

Appropriate material properties were used in the finite element model. In particular, the properties for aluminium were based on a series of test results on plate and weld metal from GRW tanker J3025 conducted by TWI. As the vast majority of the tanker consists of parent plate material and the welds are not explicitly represented in HSL's finite element model, only the parent metal test results were considered.

The bulk modulus (the compressibility of the fluid) was found not to have a significant effect on the deflection of the tanker, even for large changes in modulus. Fluid density (with associated change in volume to keep the mass constant) has a larger effect. An equivalent mass of petrol resulted in a larger deflection than water.

The behaviour of the water prior to impact was investigated using a much simplified model representing a small slice of the tanker. This model was initiated just after the point of instability (the tanker at approximately 35 degrees above the horizontal) with the surface of the water horizontal to the ground. As the tanker reached the point of impact, the surface of the water was at approximately 45 degrees.

The techniques of mass scaling (adding mass to some small elements to increase the solution speed) and Euler subcycling (solving the fluid regions of the model less frequently than the solid parts) were found to offer large benefits in terms of solution times without significantly affecting the results obtained. These approaches were adopted.

4.2 REFINEMENT AND VALIDATION OF THE TANKER ROLLOVER MODEL

4.2.1 Features of the refined finite element models

Finite element models of GRW tankers J2580 and J3910 were created, and the effect of differences between the tankers on model outputs considered. The finite element model included representation of the main shell, the extruded bands, the bulkheads and baffle, the comb along the top, and basic representations of the support structures at the front (fifth wheel location), the landing gear support and the rear. Simplified representations of the suspension, axles, steel wheels and manway covers were used. For simplicity, the finite element model used steel wheels on both sides of the tanker. Details omitted included smaller holes in the baffle, the

sumps and pump, the guttering and vapour recovery tubes through the compartments, and any other small, non-structural attachments. The basic features of the finite element model are given in Figure 18.

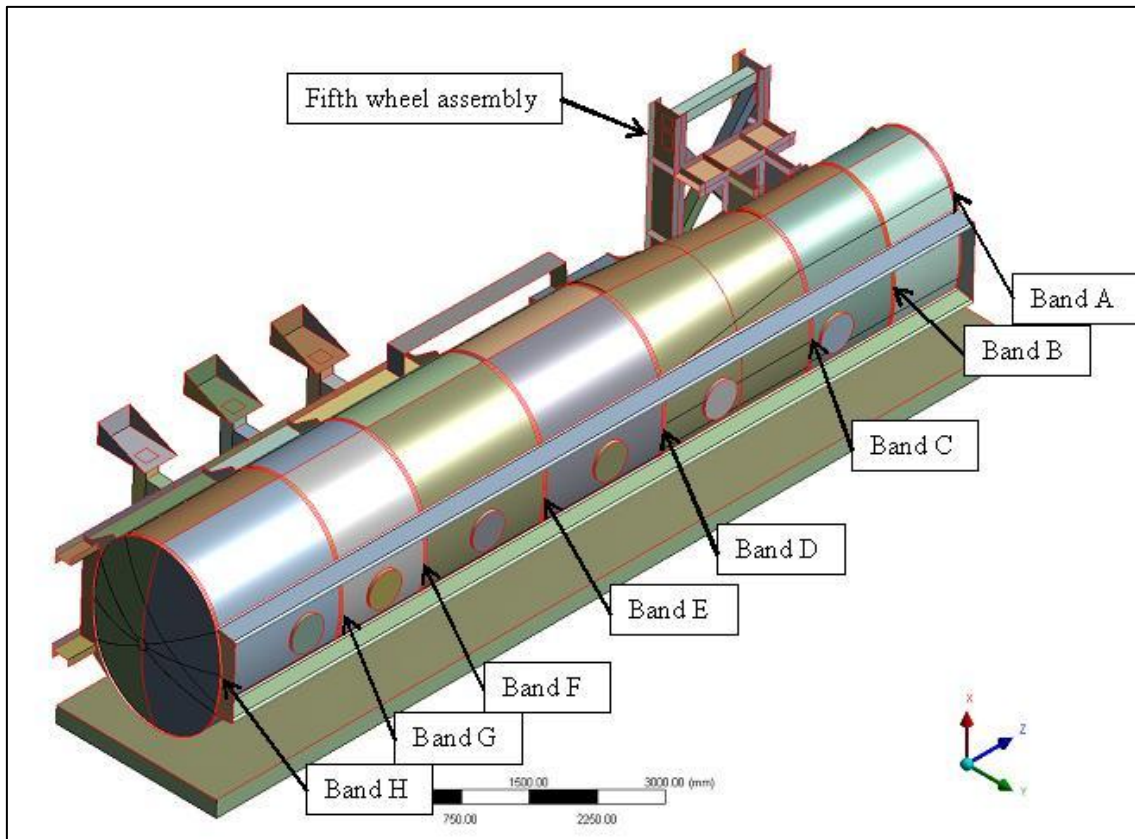


Figure 18 Overview of GRW tanker finite element model

The key differences between GRW tankers J2580 and J3910 that affected the finite element model were:

- different fillet weld locations, found during the internal weld survey before test; and
- different extrusion profiles and extrusion band welding.

Figure 19 illustrates the fillet welds in GRW tanker J3910. A long fillet weld runs to the bottom left corner - long welds were also used on GRW tanker J2580. A short (or 'stitch') fillet weld is above the strain gauge location point - these short welds were used extensively on GRW tanker J3910 but infrequently on GRW tanker J2580.

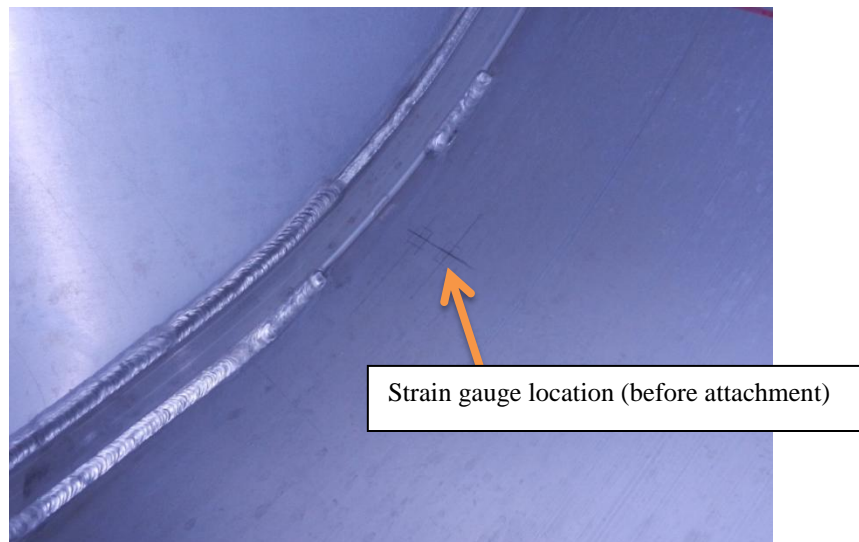


Figure 19 Fillet welds, GRW tanker J3910, Band B/8-

Figure 20 gives the extrusion profile for GRW tanker J3910, and Figure 21 gives the extrusion profile for GRW tanker J2580. In GRW tanker J2580 the bulkhead was only welded to the convex side of the bulkhead (or baffle), whereas in GRW tanker J3910 the bulkhead was welded to both sides of the bulkhead (or baffle). In addition, the extrusion was a different shape between the two tankers. If a fillet weld was present (not shown in the Figures) it would have been at the toe of the weld between the tanker shell and the extrusion.

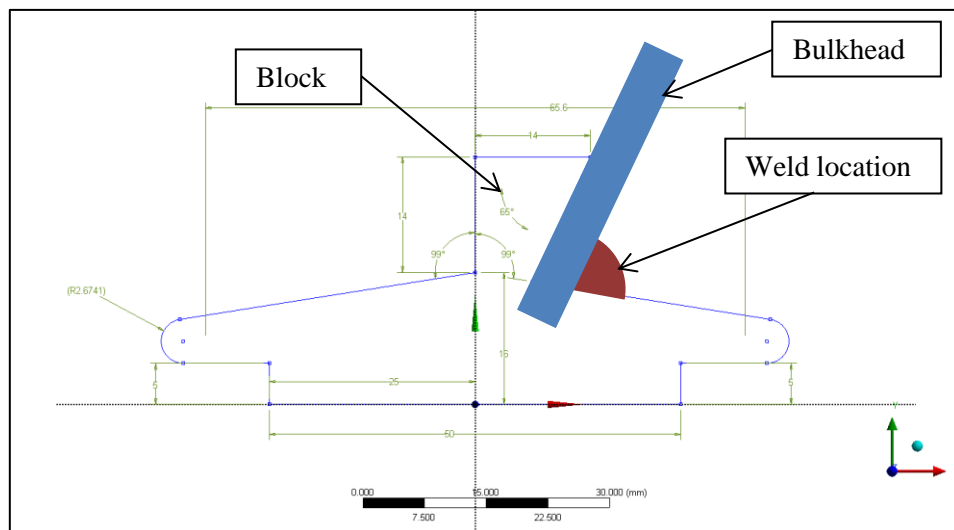


Figure 20 Band extrusion profile for GRW tanker J2580
Dimensions approximate

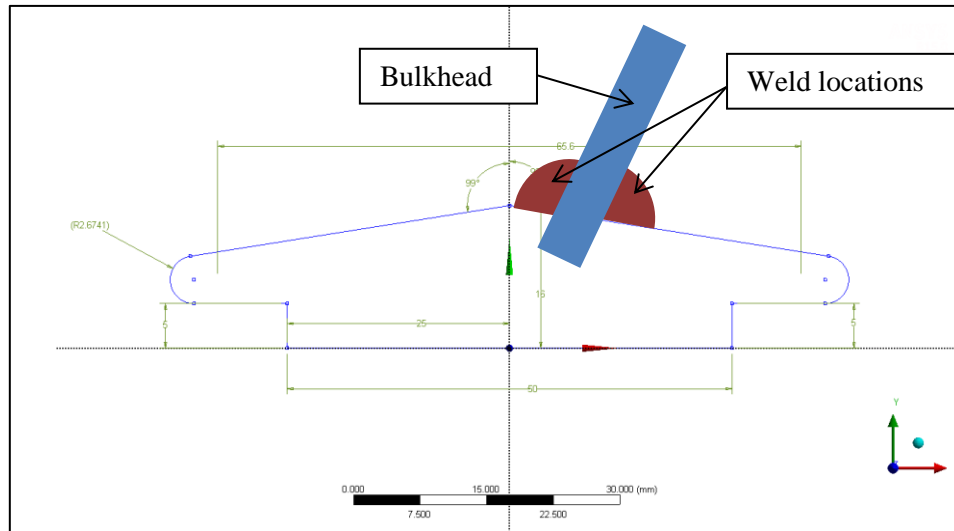


Figure 21 Band extrusion profile for GRW tanker J3910

Dimensions approximate

4.2.2 General model findings

There were only small differences between the J2580 and J3910 finite element model results. This was a similar outcome to the topple test results, which were very consistent between the tests of GRW tankers J2580 and J3910.

Impact velocity did not have a major influence on the results from the finite element analysis. This was shown both by the comparison between models using water with impact velocities of 1.89 and 2.0 rad/s, and the comparison between models using fuel oil with impact velocities of 2.0 and 2.6 rad/s. In general, the deflections/deformations and significant bending moments and membrane stresses were seen to vary by up to 10% for the cases modelled.

The orientation of the bulkheads was found to have a large effect on the bending moments in the tanker shell near to the extrusion bands. In simple terms, the bending moments were higher on the convex side of the bulkheads. In more detail, the bending moments were higher in the positive direction (putting the inner surface of the tanker shell in tension) on the convex side of the bulkheads. This was probably due to the buckling of the bulkheads during impact resulting in a slight twisting of the extruded band.

Although the resolution of the finite element model was not sufficient to consider the extrusion bands and welds in detail (this detail was considered in WP2), fillet welds were found to affect behaviour near to the extrusion bands. Results from the models suggest that internal fillet welds between the extrusion band and the shell reduce the bending moment in the shell next to the bands. It would appear that the bending moments at the shell/band interface are reduced, and not just moved to the fillet weld location. More detailed examination, with more detailed modelling of the fillet weld, would be needed to confirm the extent of the benefits of the fillet weld and the effect of intermittent, rather than continuous, fillet welds.

4.2.3 Finite element model validation

As there was little difference between the J2580 and J3910 finite element models, outputs from the J3910 model were compared to topple test data for GRW tanker J3910. Good agreement was obtained between the modified finite element model results for deformation and the topple test results based on laser scan data (Figure 22). All the flat lengths measured were within 15%, with the majority of locations showing less than 5% difference.

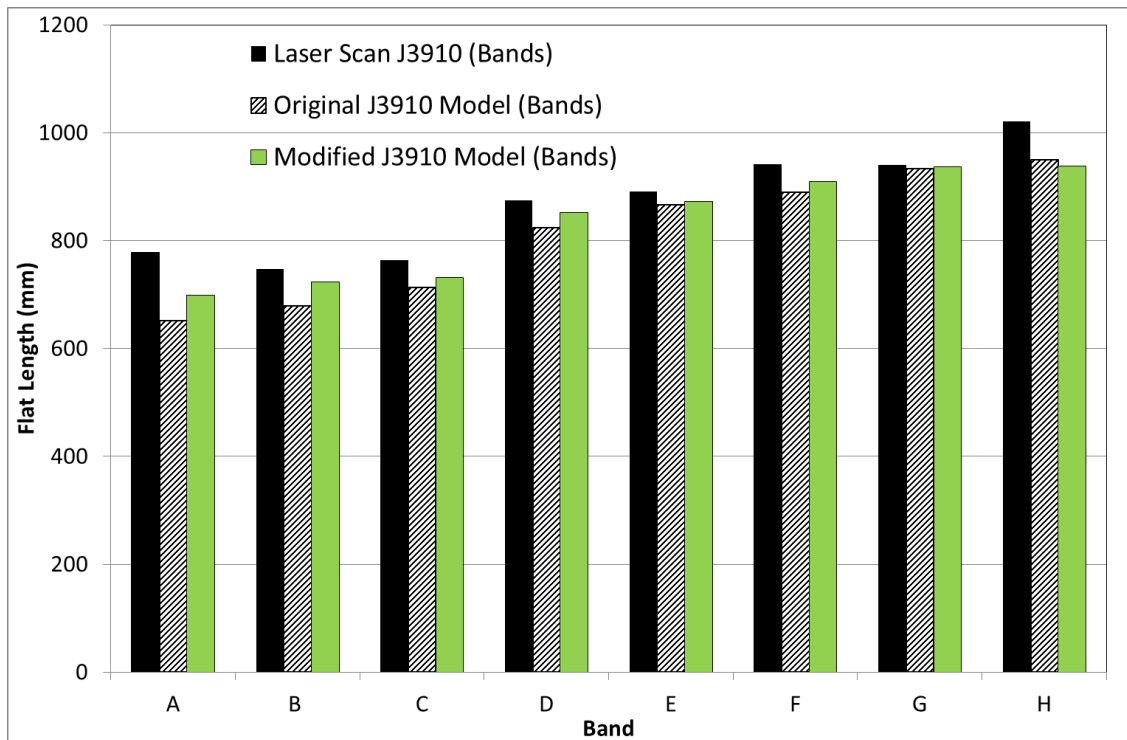


Figure 22 Comparison of flat lengths at band locations for GRW tanker J3910 test and finite element model data

The bending moments near to the extrusion bands showed generally good agreement between the test values and the finite element values. An example is given in Figure 23, and Table 4 summarises the model-to-test correlation for the bending moments and membrane stresses. (Where bending moments are expressed per unit length, the N-mm/mm units have been expressed more simply as N.) The largest difference between test and finite element model results was 22%, with most other results within a few percent. The membrane stress results showed a larger variation between test and finite element model results. Membrane stresses were generally much lower than the bending stresses at these locations, and therefore were not as important. The relative significance of the results can be more readily assessed when the differences between the test and model results are expressed as percentages of yield stress, which are included in Table 5. As can be seen, the yield stress normalisation has little effect on the bending moments (which were around yield magnitude) but significantly reduced the percentage differences for the lower membrane stresses.

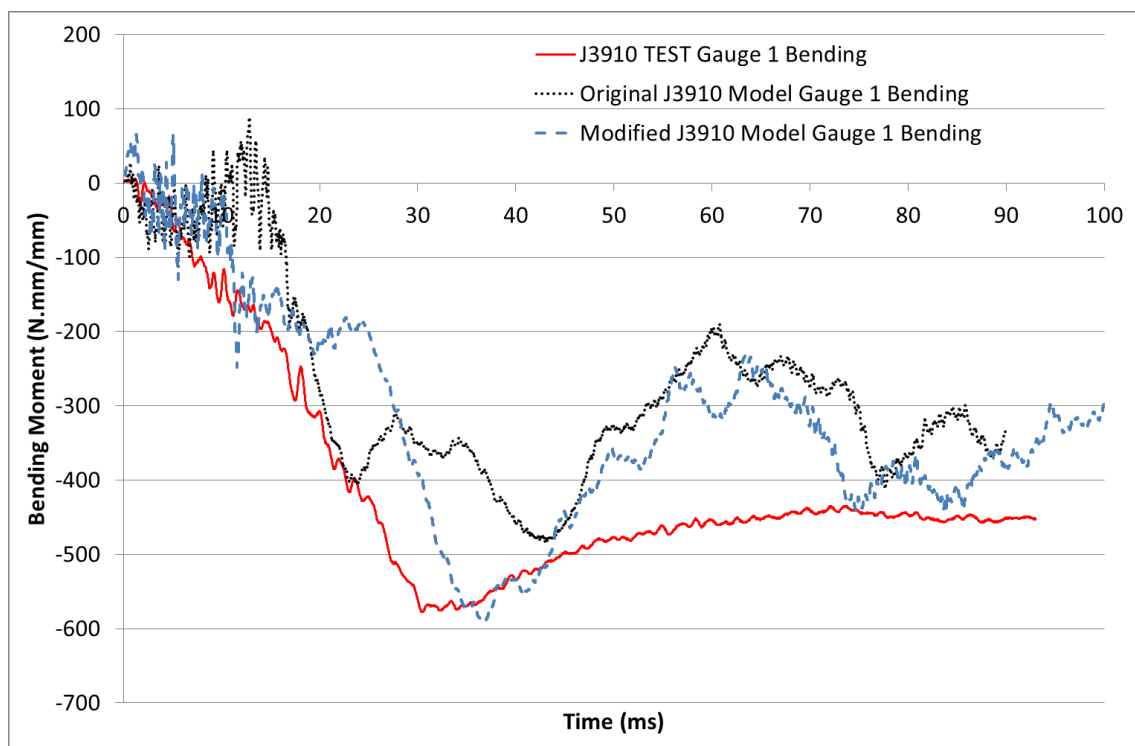


Figure 23 Comparison of bending moments near band B for GRW tanker J3910 test and finite element models

Near to band B - gauge location 1; bending moment per unit length

Table 4 Model-to-test correlation - bending moments and membrane stresses near the band with differences expressed as percentage of test result and as percentage of yield stress

Differences in bending moments and membrane stresses calculated from test data and modified finite element model for gauges near bands - where two values are reported, they are for minima and maxima

Location	Test result normalisation		Yield stress normalisation	
	Bending moment (% difference)	Membrane stress (% difference)	Bending moment (% difference)	Membrane stress (% difference)
G1 (band B)	+2	+21 / -22	+2	+4 / -7
G2 (band B)	-22	-3 / -7	-16	-0.7 / -2
G5 (band C)			-	-
G6 (band C)	-11	-20	-8	-14
G7 (band E)			-	-
G8 (band E)			-	-
G11 (band F)	-2.3	+36 / -44	-2.6	+6 / -12
G12 (band F)	-0.3	-47	-0.3	-14

The finite element models did not predict the bending stresses in the central regions of the compartments well. One of the poorest correlations is given in Figure 24. Table 5 summarises the model-to-test correlation for the bending moments and membrane stresses. In particular, bending moments in the longitudinal direction were significantly overestimated by the finite element models, although at this location, the bending moments were very small, as is evident

from the large percentage difference reductions when normalised by the yield stress. The failure of the model to predict the bending in the hoop direction in compartment 4 (gauge 9) is clear (Figure 24). However, as this location was remote from the bulkheads and the circumferential welds, the influence on the points of interest would be small.

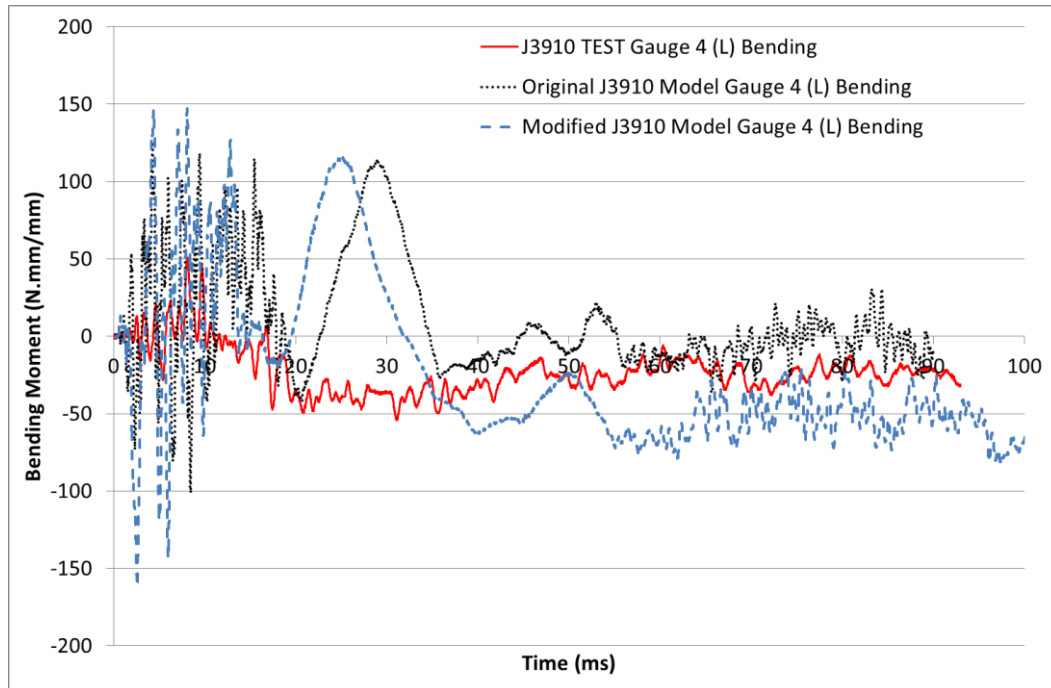


Figure 24 Comparison of bending moments at centre of C1b for GRW tanker J3910 test and finite element models

Gauge location 4 (longitudinal direction gauge at centre compartment 1b); bending moment per unit length

Table 5 Model-to-test correlation - bending moments and membrane stresses at the compartment centres with differences expressed as percentage of tests results and as percentage of yield stress

Differences in bending moments and membrane stresses calculated from test data and modified finite element model for gauges at centre of compartments - two values represent minima and maxima

Location	Test result normalisation		Yield stress normalisation	
	Bending moment (% difference)	Membrane stress (% difference)	Bending moment (% difference)	Membrane stress (% difference)
G3 (Comp 1b - Hoop)	+35 / 1	+24	+20 / +0.4	+6
G4 (Comp 1b - Longitudinal)	+194 / +188	-27	+19 / +17	-16
G9 (Comp 4 - Hoop)	-27 / -72	-30 / +10	-20 / -87	-3 / +2
G10 (Comp 4 - Longitudinal)	+61 / +88	-8	+7 / +8	-7

Good agreement was found between the pressures recorded during the test and those generated in the finite element analyses for the overall trends during the impact event (Figure 25). The magnitude of the initial pressure spikes was found, in the finite element model, to reduce rapidly

as the measurement distance from the tanker wall increased. Differences in the magnitude of the initial pressure spikes between the finite element model and test values can be attributed to difficulties in correlating the location of the finite element gauge points to the physical locations of the pressure transducers during tests.

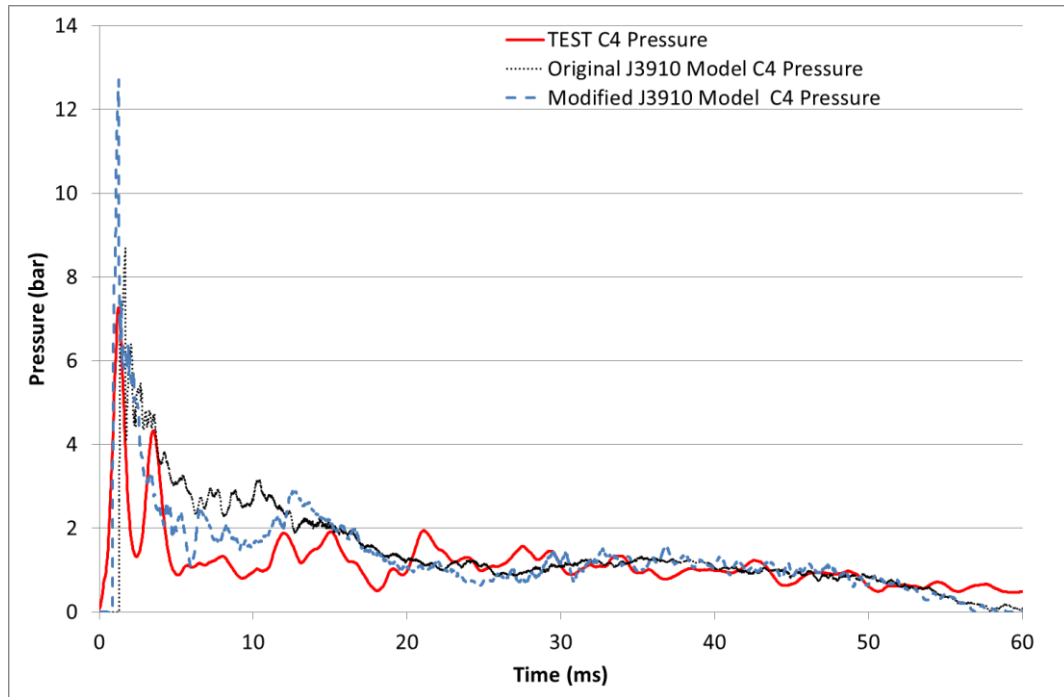


Figure 25 Comparison of pressures near the impact location in C1b for GRW tanker J3910 test and finite element model data

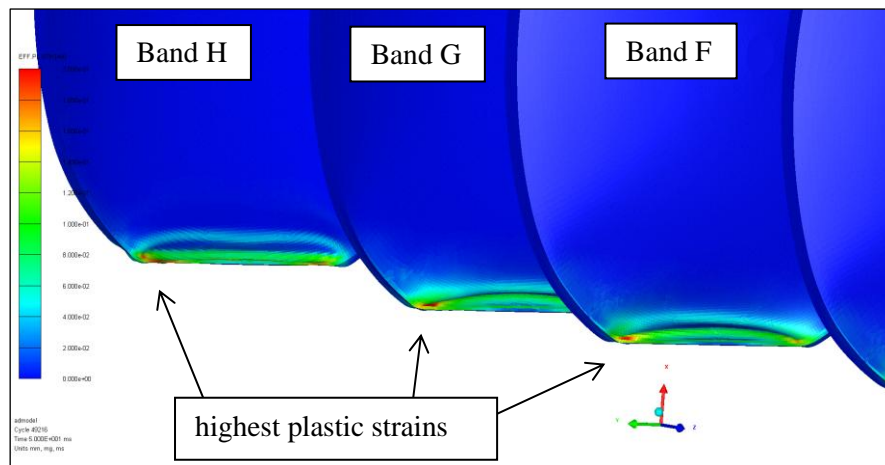


Figure 26 Plastic strain in the bulkheads from the J3910 modified finite element model

At locations on the convex side of a bulkhead where no fillet weld had been modelled, the bending moments approaching the band were typically in the order of 1,000 N-mm/mm. Where fillet welds had been modelled, the bending moments were significantly lower, with values in the order of 600 N-mm/mm. The addition of the fillet weld would thus appear to reduce the peak bending moment, rather than simply moving the peak to outside the fillet weld location.

The highest levels of plastic strain were observed in the bulkheads, at the top and bottom of the flat chord generated by the impact (Figure 26). The magnitude of the peak plastic strains was in the order of 0.2 (or 20%), a level at which failure may occur. It was at the top of this flat impact chord where ruptures in the toe of the weld and within the weld between the bulkhead and extrusion band occurred during topple tests on GRW tankers J2580 and J3910, respectively.

Overall, HSL's finite element model for J3910 correlates strongly with the topple test data for GRW tanker J3910, providing good validation for the model.

4.3 MODELLING REAL-WORLD FUEL LOADS

The model of a representative fuel oil load used a tanker with each compartment filled to its stated capacity except the third compartment from the front (the first compartment after the tanker's expanding conical section) which was empty. The empty compartment prevented the tanker being overloaded due to fuel oil's higher density than petrol, based on operator practice. The model of a representative petrol load used a tanker with each compartment filled to its stated capacity.

The compression of the front band (A/8), the rear band (H/8) and the band at the rear of the conical section (D/8) are shown in Figure 27 for water, fuel oil and petrol with impact velocities of 2.0 rad/s. Deflection at the front band shows little variation between water and fuel oil, but is greater for petrol. While behaviour at the rear of the tanker is influenced locally for fuel oil by the empty compartment, deflection was significantly higher at the rear of the tanker for fuel oil than for water, with deflection for petrol slightly higher than fuel oil. The levels of plastic strain in the bulkheads for different load liquids increase with increasing levels of deflection (Table 6). Both the through-thickness average and values near the inner surface are listed, with the strains near the surface significantly higher due to the predominantly bending nature of the strain.

Table 6 Maximum plastic strains in the bulkheads for different load liquids

Liquid	Maximum equivalent plastic strain (through- thickness average)	Maximum equivalent plastic strain (near inner surface)
Water	20 %	32 %
Fuel Oil	25 %	37 %
Petrol	34 %	41 %

It is not clear why deflections of the tanker vary so much with different liquids when the overall mass, and therefore inertia and energy, are the same. The explanation is likely to involve the different fill levels and pressure gradients within the compartments for the different liquids, and the different fill levels changing the free space above the liquid, which varies the opportunity for sloshing movement.

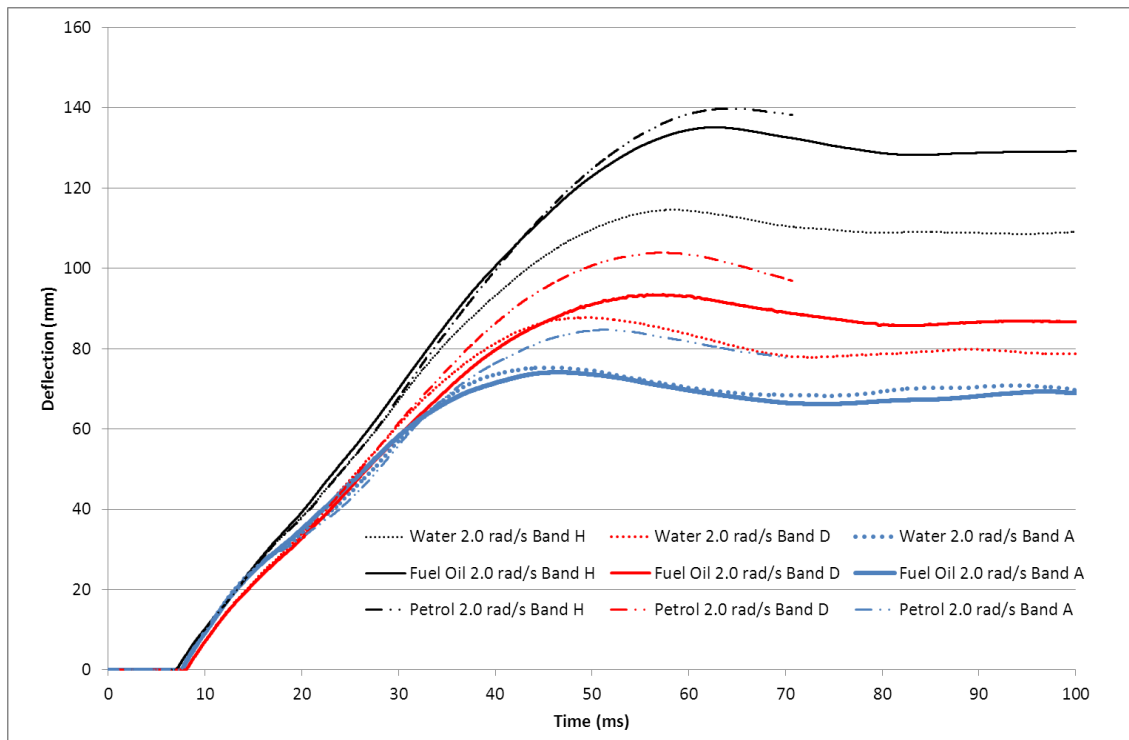


Figure 27 Effect of tanker load (fuel oil/water/petrol) on deformation (band deflections) at 2.0 rad/s impact velocity

The effect of the different liquid loads on the bending moments would appear to be highly dependent on locations. At the front of the tanker, there was little difference in the bending moments for the different liquids, although slightly higher levels of bending for petrol correspond to the higher levels of deflection for petrol.

The bending moments near to band E/8 show large differences between the models with water and petrol and the model with fuel oil (Figure 28). In the fuel oil model, compartment 3 was left empty, and band E/8 was the bulkhead separating compartments 3 and 4. Therefore, significant differences would be expected as the pressure due to the fuel oil was only acting on one side of the bulkhead.

At the rear of compartment 4 (band F/8), near the rear of the tanker, the bending moments due to the fuel oil and petrol were higher than for the water, although the trend was similar for all three liquids (Figure 29). This corresponds to the higher deflections observed at the rear of the tanker for fuel oil and petrol.

The empty compartment for fuel oil resulted in differences in the stresses in the tanker shell close to the bulkheads separating the filled and empty compartments. The deformation of the bulkhead on the front side of the empty compartment was significantly different in this model to that for water, as the pressure was only applied by fuel oil to the convex side of this bulkhead rather than to both sides of the bulkhead by water. In contrast, deformation of the bulkhead on the rear side of the empty compartment, where pressure was only applied by fuel oil to the concave side of the bulkhead, rather than to both sides of the bulkhead by water, was not significantly different in this model to that for water. This is illustrated in Figure 30. This type of deformation was not observed for the petrol model (Figure 31) where no compartment was left empty.

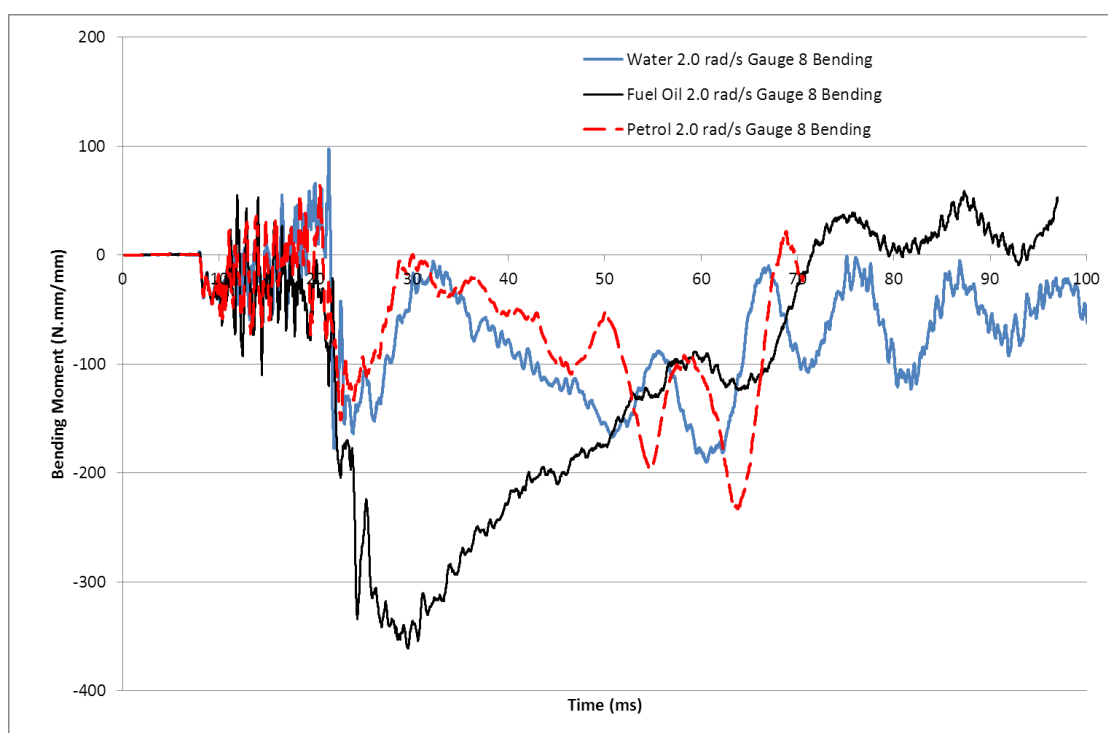


Figure 28 Bending moments near to band E showing large differences bending moment per unit length

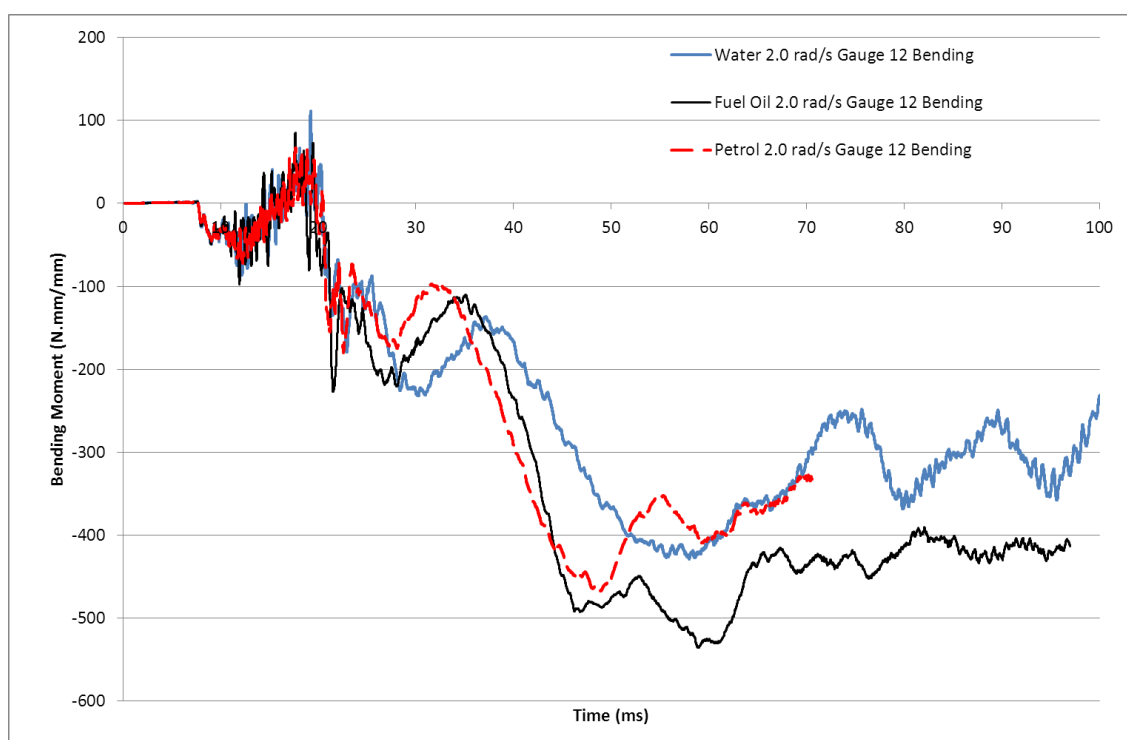


Figure 29 Bending moments near to band F bending moment per unit length

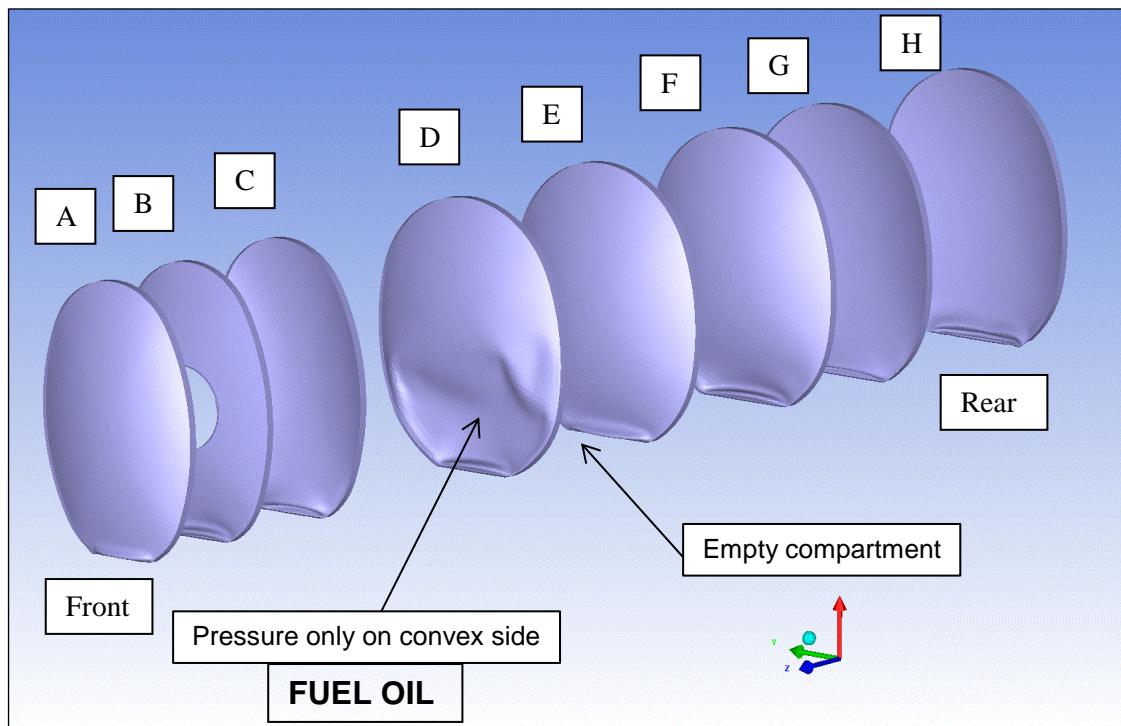


Figure 30 Deformed bulkheads for fuel oil finite element model with impact at 2.6 rad/s clearly showing effect of pressure only on the convex side of bulkhead D

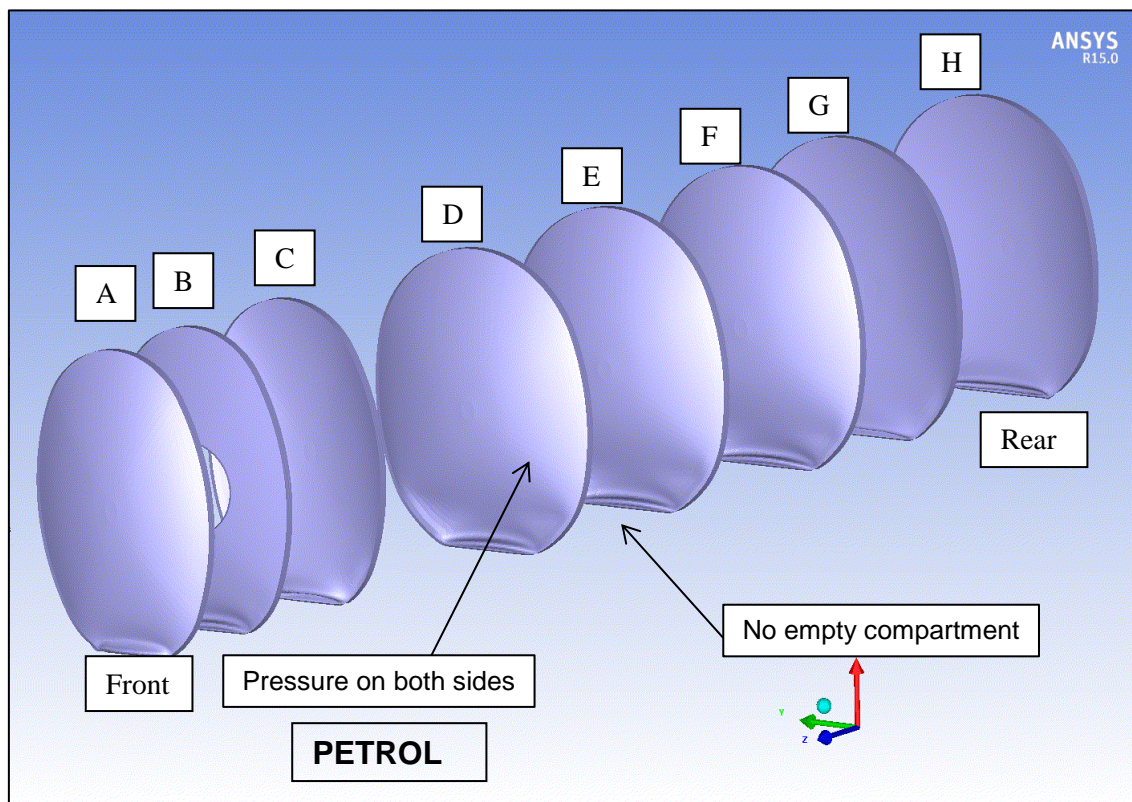


Figure 31 Deformed bulkheads due to petrol impact at 2.0 rad/s

4.3.1 Fuel load conclusions

It is clear that the behaviour of a tanker is dependent on the load that it carries. From the modelling of a tanker with full loads of fuel oil and petrol it has been shown that there is the potential for higher levels of damage to occur than if an equivalent mass of water were used. It has also been shown that loading configuration (for example, running with a compartment empty) can change the pattern of the deformation. This has been shown by the increased deflection at the rear of the tanker, the higher levels of bending moment, and the different behaviour of some bulkheads due to the empty compartment.

4.4 OUTPUT FOR WP2 ENGINEERING CRITICAL ASSESSMENT

For the WP2 engineering critical assessment (ECA) of the circumferential welds, the membrane and bending stresses acting on the joint were required. TWI created axisymmetric finite element models of the weld geometries to obtain stress intensity factor and reference stress solutions for different crack depths and weld cap geometries. The inputs for these models were bending moment and membrane stress. As these variables were more readily obtained from the tanker models than through-wall bending stresses, it was bending moments that were supplied. Also, the relationship between bending moment and through-wall bending stress was dependent on the thickness of the section at the point of interest (which was a variable in the ECA work) and the stress-strain relationship assumed.

The bending moments were highest at the rear of the tanker (Figure 32 illustrates the petrol model). The patterns and values of bending moments were very similar for the fuel oil and petrol models, with the exception of the area adjacent to band E/8, when the compartment was empty for the fuel oil model. There were areas of high bending moment within the impact zone, and also outside the impact zone close to the bands. The high bending moments here lay between the end of the impact zone and the comb, with the highest moments moving up the tanker surface as the size of the impact zone flat increased. The bending moments near to band F/8 were very similar between the fuel oil and petrol models. Figure 33 illustrates this for band F/8+, the convex side of band F/8.

In these areas, on the convex side of the bulkheads, the bending moment increased rapidly as proximity to the weld increased (Figure 34, band F/8+, the membrane stresses were comparatively low and constant with weld proximity and are not shown). Despite the large difference in the levels of deflection observed for the different liquids modelled, the maximum levels of bending moment near to the bands varied only slightly. This is likely to be due to the plastic strains in the shell limiting the level of bending moments possible. Values of bending moment and membrane stress were obtained for the weld location by extrapolating the values from the fuel oil model with an impact velocity of 2.6 rad/s. These values of 1460 N·mm/mm for bending moment and 21.5 MPa for membrane stress were supplied to TWI for the ECA. Due to the limiting effect of the plastic strains in the shell, other loading scenarios would be unlikely to give significantly different results.

During post-mortem examination of the rear of GRW tanker J2580 by TWI, a through-wall crack along the circumferential weld at the top of the impact zone in Band H+ was examined. Values of the bending moments in this area were obtained by similar extrapolation from the modified finite element model (with a water load) using the same 1.89 rad/s impact velocity as in the J2580 topple test. The results are shown in Figure 35. Bending moments at the band H+ weld plane for the locations assessed ranged from 1350 N·mm/mm to 1500 N·mm/mm. These values were supplied to TWI for the ECA, and were similar to those obtained for the fuel cases at Band F+.

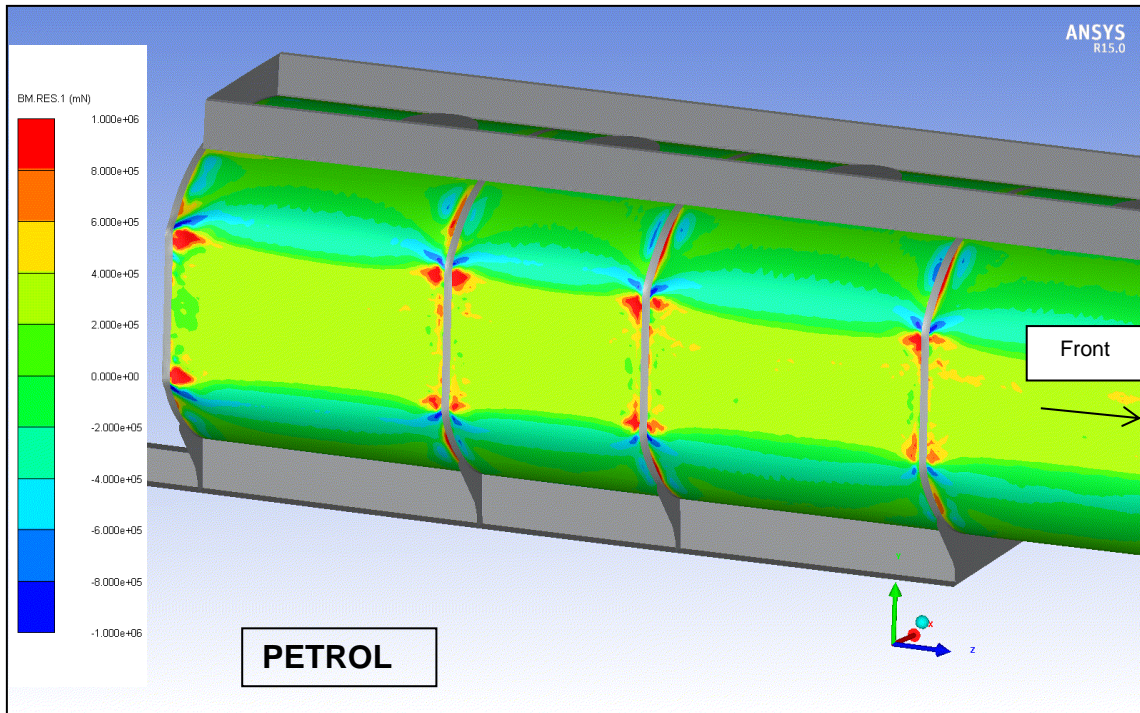


Figure 32 Bending moments per unit length at the rear of the tanker shell under petrol loading conditions at 2.0 rad/s (for clarity, moments in other components not shown)

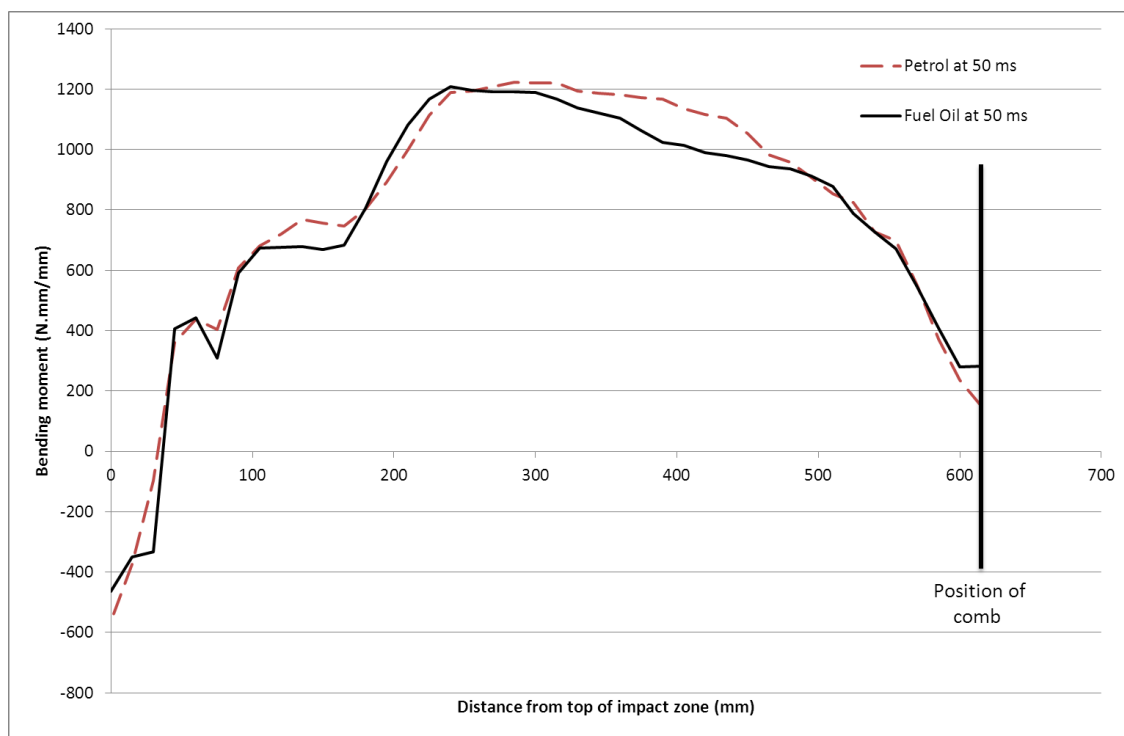


Figure 33 Bending moments next to Band F/8+ showing variation due to fuel (petrol 2.0 rad/s, fuel oil 2.6 rad/s)

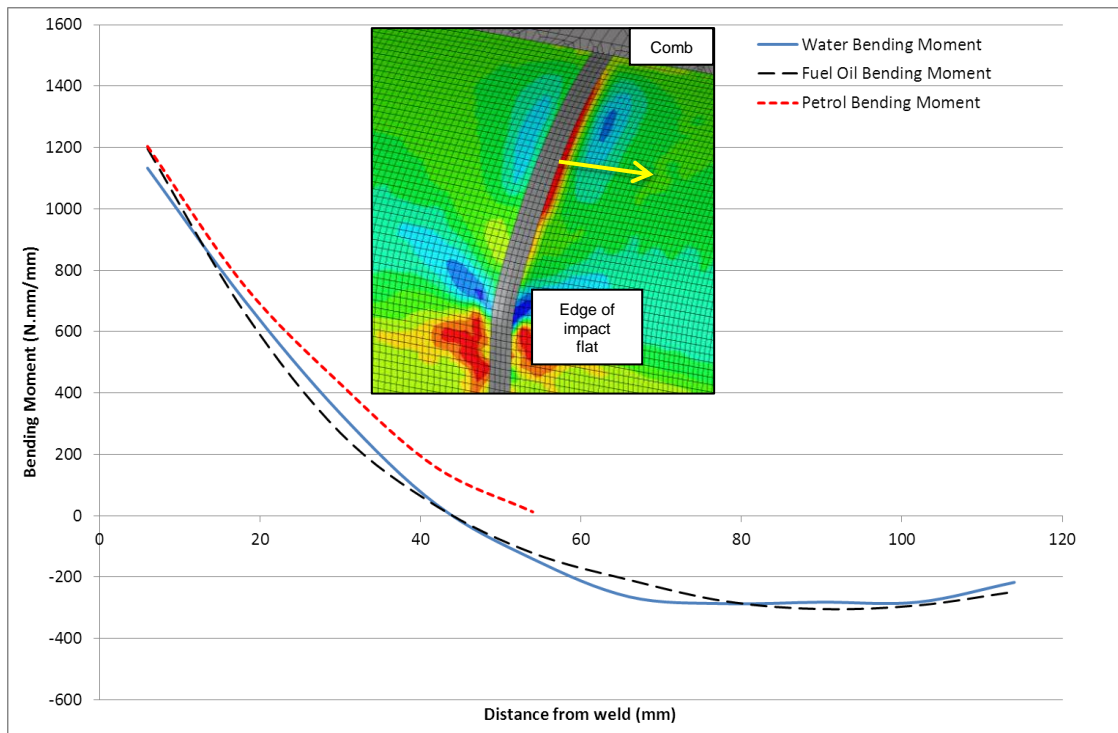


Figure 34 Variation in bending moments with distance from the weld (Band F/8+) for water (2.0 rad/s), fuel oil (2.6 rad/s) and petrol (2.0 rad/s)

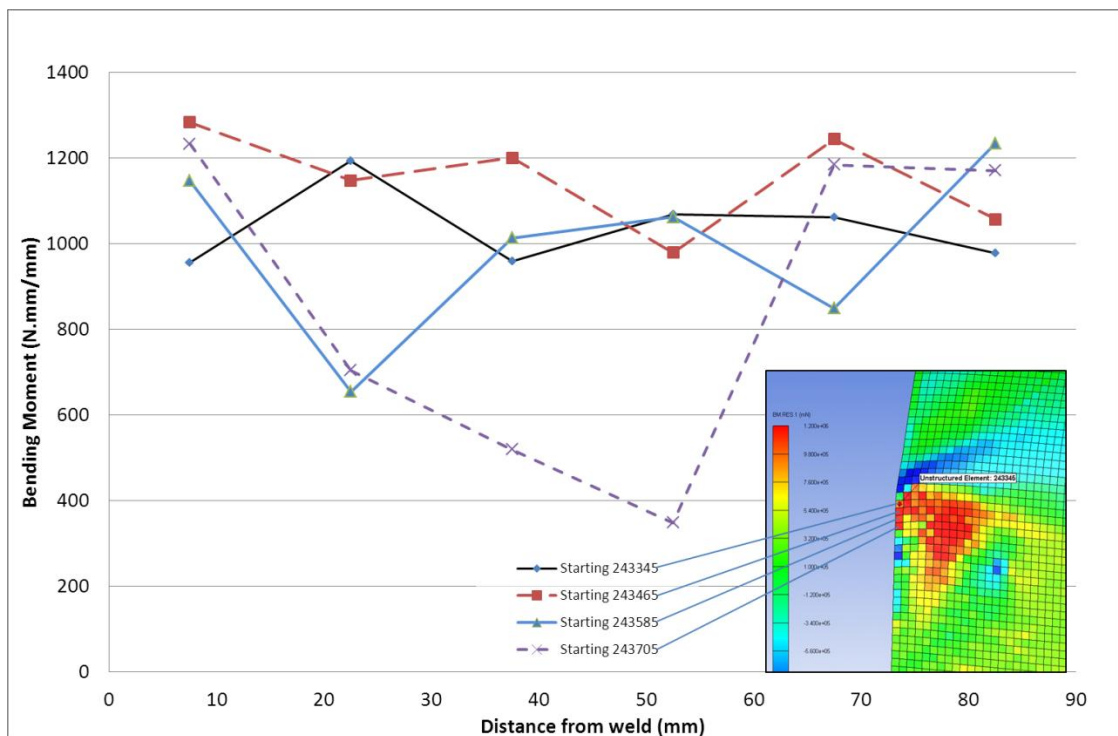


Figure 35 Variation in bending moments with distance from the rear weld (Band H+) for water at 1.89 rad/s

5 CONCLUSIONS

Overall findings

The test outcomes demonstrated that the topple test was a reliable test method providing repeatable test data suitable for validating HSL's Finite Element (FE) modelling. The impact velocities for the GRW tanker tests lay within the range reported for real-world rollovers.

Overall, HSL's finite element model of the HSL topple test with a water load for GRW tanker J3910 correlated well with the topple test data, providing good validation of the model.

The highest levels of plastic strain in the finite element model with a water load were observed in the bulkheads, at the top and bottom of the flat generated by the impact. The magnitude of the peak plastic strains was in the order of 0.2 (or 20%), a level at which failure may occur. It was at the top of this flat where ruptures in the toe of the weld and within the weld between the extrusion band and the bulkhead occurred during the topple tests on GRW tankers J2580 and J3910, respectively.

Assessment and supply of tankers

The primary criteria for GRW tanker selection, for both the topple tests (WP1) and the fatigue data collection activities (WP2) were:

- that the tanker should be representative of 'in-service' UK-based GRW tankers; and
- the condition, based on radiography, of the tanker's circumferential welds to ensure the tests included a range of weld qualities of tankers as found in service.

The circumferential welds of ten⁵ 8- and 10-banded GRW tankers manufactured between 2007 and 2011 were radiographed (four prior to the project). The results of the radiography both informed the selection of tankers for the topple and road tests, and provided information on the condition of the welds in a range of GRW tankers manufactured over a five-year period. Two 8-banded 6-compartment tankers, J2580 and J3910, were selected for topple tests. One 10-banded 6-compartment tanker, J3857, was selected for road tests to gather fatigue data in WP2. The radiography for J3910 showed the highest proportion of lack of fusion indications in the welds, whilst J3857 and J2580 showed the lowest.

The GRW tankers selected for test were all fully ADR inspected and, where necessary, remedial work was conducted to ensure that the tankers satisfied the test requirements, and were roadworthy and loadworthy. In addition, the GRW tankers selected for topple test were subject to a second radiography examination, and to internal surveys of the fillet welds. GRW tanker J3910 was subject to an additional internal survey of circumferential weld misalignment, and an external laser scan survey of the circumferential weld caps. General design and construction differences between 8- and 10-banded tankers, which were relevant to the research, have been established. Specific design and construction differences, due to changes in GRW design and welding process, between GRW tankers J2580 and J3910 were found in the extrusion profiles, the bulkhead (or baffle) welding to the extrusion bands and the fillet welds.

A suitable 8-compartment 40,000 litre petroleum road tanker of aluminium construction in roadworthy and loadworthy condition was sourced for the proof of concept topple test. Two damaged GRW tankers, J3217 with rear damage and J3146 with front damage, were laser scanned for dimensional information on the damage, with physical samples taken, for WP2 use.

⁵ one further tanker may be added to the list in a revision of this report

Tanker topple test methods and results

Overall, the outcomes of a proof of concept test and tests on two GRW tankers, J2580 and J3910, demonstrated that the topple test was a reliable test method providing repeatable test data suitable for validating HSL's finite element modelling.

HSL developed a topple test with a water load whereby a prepared tanker was tilted under controlled conditions until it became unstable and fell onto its offside under the influence of gravity. GRW tankers were instrumented with pressure transducers, strain gauges and accelerometers to record data for the impact, logged at 50,000 samples per second (or one sample every 0.02 millisecond). Tests were recorded using thirteen video cameras ranging from standard speed (25 frames per second) to high speed (1,000 frames per second).

GRW tankers J2580 and J3910 were filled to be at, or very close to, their maximum rated load mass (31,380 kg), which was below their rated volume for fuel. Both were filled with 31,376 litres of water (31,376 kg), with each of their compartments filled to about 70% of its maximum capacity. The impact velocities for the GRW tanker tests were between 1.82 and 1.93 rad/s, values which lie within the range of 1.75 to 2.62 rad/s reported for real-world rollovers. The offside of the tanker impacted uniformly along its length, with less than 7 ms between the impact of the front and rear for the GRW tankers.

After the test, the offside (impact side) of the GRW tankers exhibited a similar deformation shape with the impact area flattened. The deformation profile was similar along the length of the tankers, with the level of deformation increasing from front to rear. The deformation data, both as a reduction in tanker diameter and as the chord length of the flat section, were similar for the GRW tankers. The impact caused a permanent reduction in tanker diameter of approximately 100 mm at the rear and 82 mm at the front of GRW tanker J2580, and of approximately 107 mm at the rear and 82 mm at the front of GRW tanker J3910.

GRW tankers J2580 and J3910 both ruptured during impact. There was a visible leak from GRW tanker J2580 between the rear bulkhead and extrusion band at the top of the impact area. Subsequent visual inspection found a rupture within the weld between the rear bulkhead and extrusion band at the top of the impact area, and no visible damage at the bottom of the impact area. Pneumatic pressure tests found that all compartments in GRW tanker J2580 had lost their internal integrity. HSL supplied TWI with samples from GRW tankers J2580 and J3910 for post-mortem assessment under WP2. During post-mortem examination, TWI observed an apparent through-wall crack along the circumferential weld at the top of the impact zone for the sample including the impact zone from the off-side rear of GRW tanker J2580. This apparent crack can be seen on close examination of HSL photographs of the tanker after being lifted back onto its wheels. Detailed fractographic analysis of the J2580 and J3910 samples is addressed in the WP2 report. GRW have indicated that the damage around the joints between the extrusion band and the bulkhead/baffles for both tankers is consistent with real-world rollovers.

There was a visible leak from GRW tanker J3910 between the front bulkhead and the extrusion band at the top of the impact area. Subsequent visual inspection found a rupture in the toe of the weld between the front bulkhead and the extrusion band at the top of the impact area, and a crack in the toe of this weld at the bottom of the impact area. Pneumatic pressure tests of GRW tanker J3910 found that internal integrity had been lost between compartments 1 and 2 and between compartments 4 and 5, while the other bulkheads and compartments had maintained their internal integrity.

Modelling to provide load case data for rollover

Overall, HSL's finite element model of the HSL topple test with a water load for J3910 correlated well with the topple test data for GRW tanker J3910, providing good validation of the model. There were only small differences between the finite element model results for J2580 and J3910. This was a similar outcome to the topple test results, which were very consistent between the tests of GRW tankers J2580 and J3910. The highest levels of plastic strain in the finite element model with a water load were observed in the bulkheads, at the top and bottom of the flat generated by the impact, with peak magnitudes in the order of 0.2 (or 20%), a level at which failure may occur. It was at the top of this flat where ruptures in the toe of the weld and within the weld between the bulkhead and extrusion band occurred during the topple tests on GRW tankers J2580 and J3910, respectively.

The orientation of the bulkhead curvature was found to have a large effect on the bending moments in the tanker shell near to the extrusion bands. In simple terms, the bending moments were higher on the convex side of the bulkheads. Although the resolution of the model was not sufficient to consider the extrusion bands and welds in detail (this detail was considered in WP2), fillet welds were found to affect behaviour near to the extrusion bands. Impact velocity within the ranges modelled (1.89 to 2.0 rad/s for water, 2.0 to 2.6 rad/s for fuel oil and 2.0 rad/s for petrol) did not have a major influence on the results from the finite element models.

The fuel oil case modelled the tanker with one compartment empty, as occurs in practice because fuel oil has higher density than petrol. Modelling a tanker with a representative load of fuel oil or petrol, as opposed to water in all compartments, led to significantly higher deformation at the front of the tanker for petrol, and at the rear of the tanker for both fuels. Pressures, stresses and bending moments for the fuel oil and petrol models were also higher at the rear of the tanker than for the water model. The most significant feature for fuel oil was the behaviour around the empty compartment, with considerable differences when compared to the water model. The fuel load models suggest that the topple test conditions, with a water load distributed evenly throughout the tanker, may not be as severe as some real-life events.

Using the 2.6 rad/s fuel oil model, single values for bending moment (1460 N-mm/mm) and membrane stress (21.5 MPa) at the front side of the rear extrusion band in compartment 4 were extrapolated from model elements close to the circumferential weld. Extrapolating the same way using the 1.89 rad/s water model gave bending moments up to 1500 N-mm/mm for the location on the rear circumferential weld of compartment 6 corresponding to the through-wall crack in GRW tanker J2580. These values were supplied to WP2 for the detailed ECA. The limiting effect of the plastic strains in the shell means that other loading scenarios would be unlikely to give significantly different results.

6 REFERENCES

- [1] EN ISO 10042: 2005, Welding. Arc-welded joints in aluminium and its alloys. Quality levels for imperfections.
- [2] European Agreement on the Carriage of Dangerous Goods by Road (ADR) (2013).
Website information correct on 29 August 2014:
<http://www.unece.org/trans/danger/publi/adr/adr2013/13contentse.html>
(summary information can be found on the HSE website at:
<http://www.hse.gov.uk/cdg/manual/adrcarriage.htm>)
- [3] B.J. Robinson, T. Robinson, M Tress and M. Seidl, 'Technical Assessment of Petroleum Road Fuel Tankers - Accident Data and Regulatory Implications' TRL Project Report RPN2925, 2014
- [4] I.N. Bysh and M.R. Dorn '*The generation of internal pressure in tanker rollover*', HSE Contract Research Report No 109/1996.